X-672-65-313

NASA TM X-55280

AIMP
SUMMARY DESCRIPTION

GPO PRICE $ _____

CSFTI PRICE(S) $ _____

Hard copy (HC) 3.00

Microfiche (MF) .50

ff 653 July 65

AUGUST 1965

NASA — GODDARD SPACE FLIGHT CENTER —

GREENBELT, MARYLAND

X-672-65-313

AIMP
SUMMARY DESCRIPTION

GODDARD SPACE FLIGHT CENTER
Greenbelt, Maryland

Prepared by: J. J. Madden
J. J. Madden

Approved by: P. G. Marcotte
P. G. Marcotte

BLANK PAGE

CONTENTS

AIMP SUMMARY DESCRIPTION

TECHNICAL PLAN

INTRODUCTION

Objectives

The primary objective of the AIMP (IMP D&E) project is to investigate in the vicinity of the moon the characteristics of the interplanetary magnetic field, solar-plasma flux, interplanetary dust distributions, solar and galactic cosmic rays, as well as to study the magnetohydrodynamic wake of the earth in the interplanetary medium at lunar distances every 29.5 days.

Secondary objectives of the AIMP project, accomplished by analyzing respectively the dynamics of the satellite's orbit and the variations of its telemetry signal, are to provide information on the lunar gravitational field (for investigating the mass distribution of the moon, the earth-moon mass ratio, and the figure of the moon), and on any possible lunar ionosphere by observing radio-wave propagation from the vicinity of the moon.

Approach

Until now, space probes and earth-orbiting satellites have furnished the only direct measurements of the physical properties and dynamic characteristics of the interplanetary medium. Both methods have produced valuable information; however, each is limited in certain areas of investigation. The space probe, limited to a single data-collecting pass along a selected trajectory, provides little information on dynamic characteristics. Satellites in near-earth orbits supply the repetitive monitoring required to determine the dynamics of this portion of the interplanetary medium; however, the geomagnetic field, which dominates the phenomena under investigation in this area, drastically modifies certain characteristics of the interplanetary medium, thereby limiting the usefulness of the data. In high-altitude orbits, earth satellites can monitor conditions outside the disturbing influence of the earth's magnetic field, but like space probes, have limited ability to monitor rapidly changing conditions because of the length of time between comparable passes.

The lunar-anchored satellite is an improved means of achieving program objectives since it traverses the sunlit and night sides of the earth once every 29.5 days. In addition, the spacecraft in a lunar orbit will provide direct measurements of the dust flux in the vicinity of the moon and may provide information on certain physical properties of the moon and on its ionosphere.

Current studies indicate that a lunar orbit inclined between 140 and 180 degrees to the moon's equator, having an apocynthion less than 46,000km and a pericynthion greater than 500km, is acceptable for probability of success and lifetime criteria; however, a more desirable set of orbital parameters can be obtained through proper selection of fourth-stage (retromotor) firing time. The actual orbit, within the ranges selected, will be determined by the firing time of retromotor, which will be determined from an analysis of the actual transfer trajectory attained. The project office will use real-time trajectory tracking data to select the firing time with the best set of orbital parameters for meeting project constraints (life, spin-axis/sun-angle, and shadow conditions) and scientific objectives.

The AIMP-D spacecraft will be launched from the Eastern Test Range (ETR) during the calendar year 1966 into a transfer trajectory by a thrust-augmented improved Delta (DSV-3E) and an X-258 third stage. The retromotor, a Thiokol TE-M-458, will slow the spacecraft to permit its capture by the lunar gravitational field.

The Delta project office and the Systems Analysis Office are preparing independent launch-window studies. The Delta project office studies are primarily vehicle-oriented; the systems analysis office studies ground support-oriented. Both offices, using different computer programs, will run complete mission studies, cross checking information in pertinent areas.

Douglas Aircraft Company (DAC), under the direction of the Delta project office, will conduct a mission analysis and will prepare an optimized nominal flight plan based on the Delta vehicle capabilities. The DAC studies will be thoroughly checked by both the Delta project office and the Systems Analysis Office. Figure 1 is a typical flight plan.

EXPERIMENTS

Radiation Experiments

The AIMP complement of experiments includes three radiation-monitoring experiments:

- The energetic particle [illegible] experiment conducted by the University of California—K. A. Anderson, investigator
- The electron and proton experiment conducted by the University of Iowa—J. A. Van Allen, investigator

- The plasma probe conducted by the Massachusetts Institute of Technology—H. S. Bridge, investigator

Figure 2 illustrates the energy ranges investigated by each of the experiments; Figure 3 shows experiment view angles.

Energetic-Particle Experiments (University of California)—A list of the scientific objectives follows:

- Search for low-energy solar electrons in interplanetary space. Fluxes as small as about $3\,cm^{-2}\ sr^{-1}\ sec^{-1}$ will be detectable. The main interest here is with electron fluxes inside gas clouds which produce magnetic storms. If this aspect of the experiment is negative at least a very small lower limit will have been set.

- Low-energy protons can be detected and the relation of these to storm producing solar plasma will complement the electron measurement.

- The flux of terrestrial electrons and protons sluffed off the magnetosphere which appear near the moon will be monitored. The frequency of appearance and intensity of energetic electrons in the geomagnetic tail will be monitored $60\,R_e$ from the earth.

- The ion chamber will provide a precise and sensitive monitor of changes in the galactic cosmic ray intensity of all time scales down to 6 minutes or so.

- The counters will provide a time history of solar cosmic ray events over three integral energy regions:

  GM 1 $\geq$ 50 kev
  Ion chamber $\geq$ 17 Mev
  GM 2 $\geq$ 0.5 Mev

  Spectral changes will appear as changes in the ratios of the three integral rates.

Of considerable practical interest in connection with solar cosmic-ray events observed on the lunar anchored IMP satellites will be the properties of the moon as a particle shield. Whether or not particles are excluded from the antisolar surface of the moon can be answered for the above three energy intervals, each as a function of time. Of further practical interest is the fact that the ion chamber inherently converts the particle spectrum to a dose rate measurement. It is planned that the shielding will be about $0.4\,g\,cm^{-2}$.

ANCHORED IMP LAUNCH SEQUENCE

SEQUENCE NO.	TIME/SEC	EVENT
1	0	STAGE I LIFTOFF
2	148	MAIN ENGINE CUTOFF
3	152	STAGE II IGNITION SIGNAL
4	153	STAGE I/II SEPARATION
5	215	JETTISON FAIRING
6	542	STAGE II CUTOFF
7	562	START COAST PHASE PITCH PROGRAM
8	1099	END COAST PHASE PITCH PROGRAM
9	1104	FIRE SPIN ROCKETS (SPIN UP)
10	1106	JETTISON STAGE II-ACTIVE RETRO SYSTEM
11	1110	STAGE III IGNITION
12	1132	STAGE III BURNOUT
13	1179	DE-SPIN STAGE III/SPACECRAFT
14	1227	SOLAR CELL PADDLE RELEASE (4)
15	1229	FLUXGATE BOOM RELEASE (2)
16	1234	SPACECRAFT/STAGE III SEPARATION-YO STAGE III
17		SPIN STABILIZED COAST
18	DBC	COMMAND TIMER
19	DBC+T	DIRECT COMMAND STAGE IV IGNITION
20	DBC+T+22	STAGE IV BURNOUT
21	DBC+T+22+1200+	SEPARATE STAGE IV
22		IN ORBIT

T=TIMER
DBC=DETERMINED BY COMPUTER

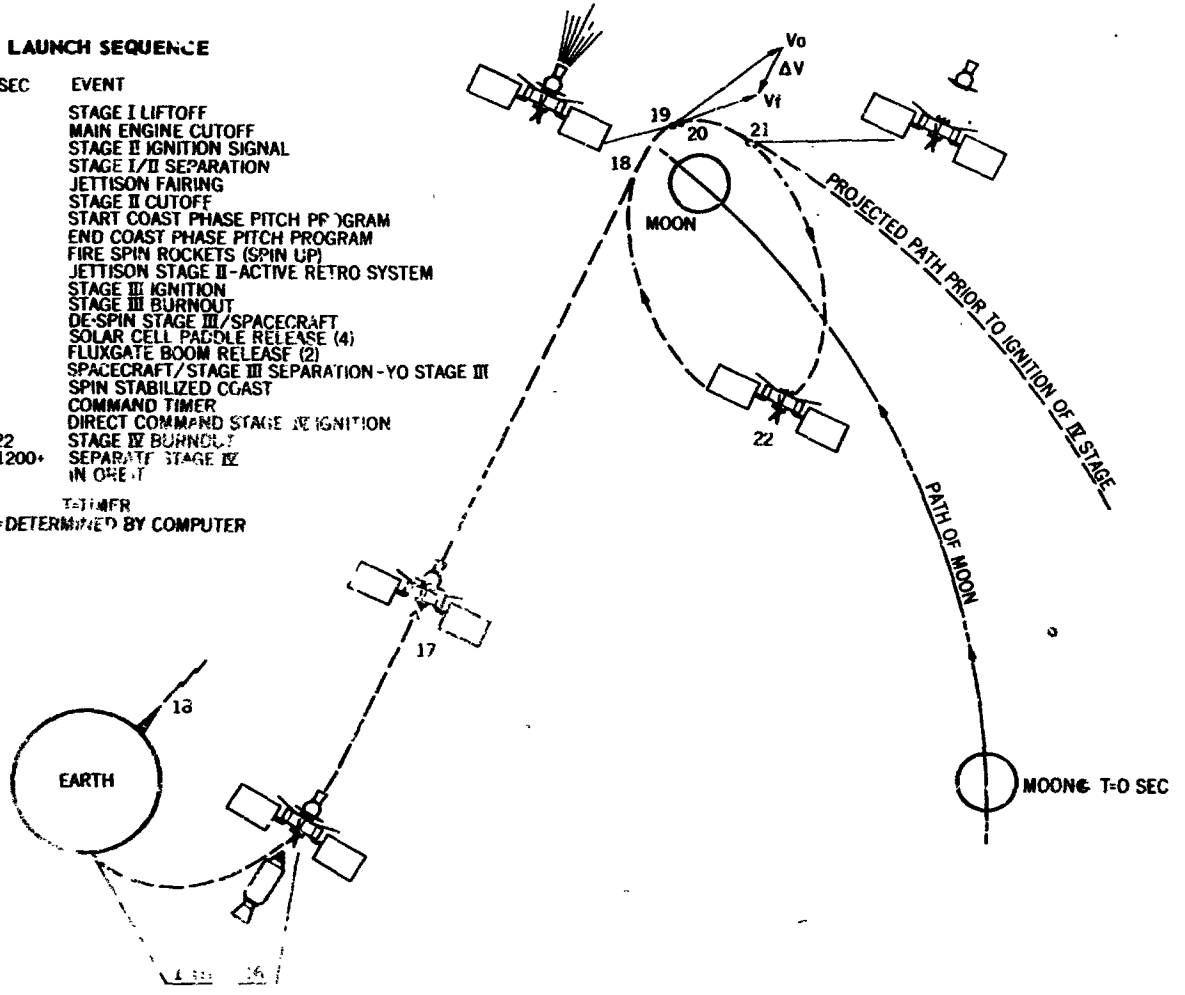

Figure 1. Typical Flight Plan

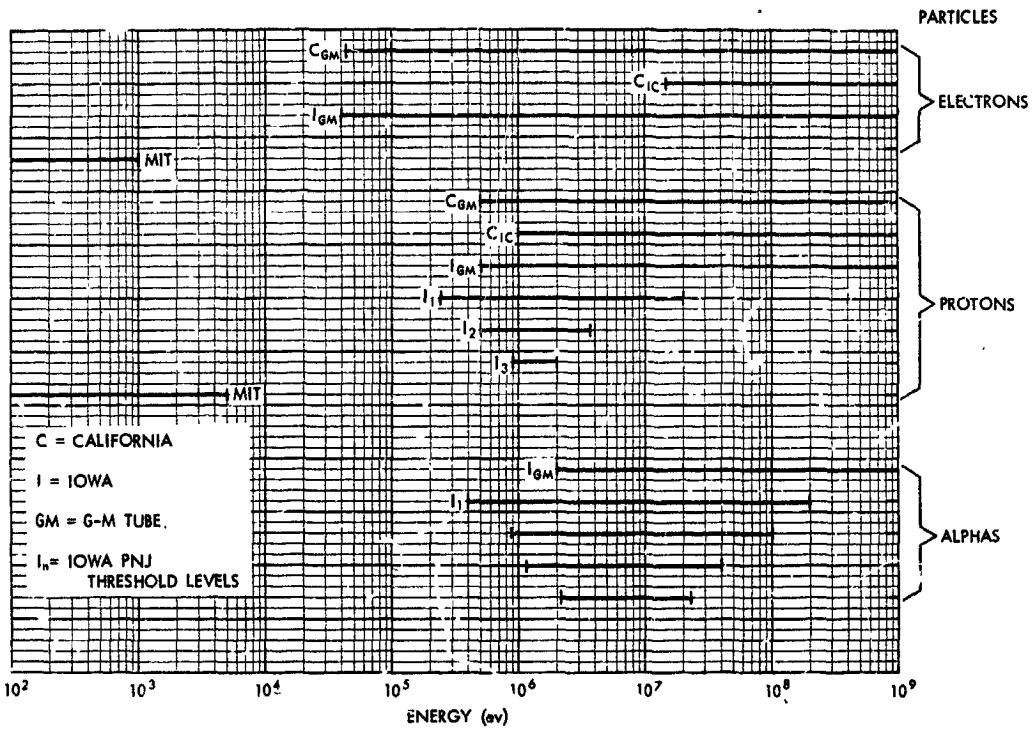

Figure 2. Radiation Experiment Energy Ranges

The monitor apparatus (ion chamber and two GM tubes) will be essentially the same as that flown on IMP-B and IMP-C.

Electrons and Protons Experiment (University of Iowa)—The objectives of this experiment are:

- To study the spatial, temporal, and angular distribution of electrons with energies exceeding 40 kev in the magnetospheric wake of the earth at 60 earth radii (60 R_e)
- To search for electrons with energies exceeding 40 kev in the wake of the moon, and to conduct a detailed study of their distribution if workable intensities are found
- To study the incidence and intensity of low-energy solar cosmic rays versus time profile (protons and alpha particles separately) in interplanetary space, and to determine their energy spectra and angular distribution
- To study solar X-rays in the 0-14 angstrom range

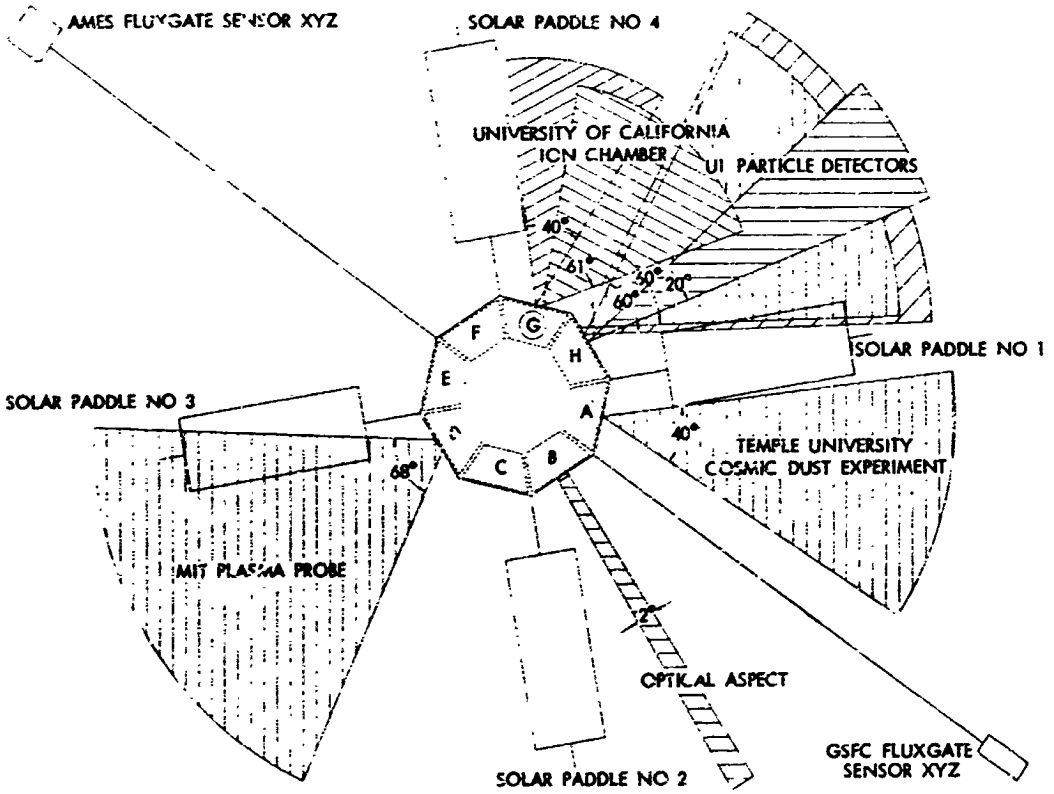

Figure 3. Experiment View Angles

To accomplish these objectives, three GM tubes and one PNJ are used. The GM tubes are eon type 6213 with 1.2 mg/cm^2 mica windows. All three have the same characteristics except for view angle. The collimator for GM 1 is fan-shaped with a 12-degree full angle in the meridian plane and a 30-degree full angle in the equatorial plane of the spacecraft. The collimator of GM 2, a circular cone with a 25-degree half-angle, has its axis parallel to the spin axis. The collimator for GM 3, also a circular cone with a 25-degree half-angle, has its axis parallel to the spacecraft spin axis but directed oppositely to that of GM 2. The PNJ, a totally depleted surface-barrier silicon detector about 25 microns thick, has its axis in the equatorial plane of the spacecraft and passes through the rotational axis. Its view angle takes the form of a circular cone with a 30-degree angle.

Plasma Probe (Massachusetts Institute of Technology)—The experiment is designed to measure the following:

- Angular distribution of the total proton flux in the equatorial meridian plane of the spacecraft

- Energy distribution of the proton flux at or near the same angle as the peak of the total proton flux

- Angular distribution of the electron flux in the equatorial and meridian plane of the spacecraft

- Energy distribution of the electron flux at or near the same angle as the peak of the total electron flux

The sensor is a current collector of the MIT Faraday cup variety mounted so that its direction of view is at right angles to the spin axis of the vehicle. The sensor has an acceptance cone of 68 degrees. As the sensor rotates with the spacecraft, the variation of the signal with time is determined by the directional characteristics of the plasma in the equatorial plane and by the angular acceptance function of the sensor itself. In particular, the sensor is designed to measure the energy spectrum and angular distribution of the proton and electron flux of the plasma at specific increments in the range of 100 ev to 5 kev.

Ames Magnetometer

The Ames magnetometer experiment consists of a boom-mounted sensor unit located approximately 7 feet from the center of the spacecraft perpendicular to the spin axis, and the magnetometer electronics located in the equipment area. The sensor unit consists of three orthogonally mounted individual fluxgate sensors (x, y, and z). Sensors x and y are mounted perpendicular to the spin-axis; sensor z parallel to the spin-axis. A flipper system rotates sensors x and z 90 degrees once each day to reorient sensor position for calibration.

The system is designed to measure the spatial and temporal variations of the interplanetary and lunar magnetic fields in 3 linear ranges covering the 0.2- to 200-gamma range.

The on-board data-processing system uses a synchronous demodulation process to maintain the spacecraft coordinate system, and data-compression techniques to provide a more constant output accuracy over the dynamic range of the system. The output of the data-processing system is presented in analog form to the spacecraft encoder.

GSFC Magnetometer

The GSFC magnetometer experiment is also a boom-mounted three-component fluxgate magnetometer provided with a flipper mechanism.

The orthogonally mounted sensors are arranged with one sensor parallel to the spin axis of the spacecraft and the remaining two perpendicular to the spin-axis. A flipper reorients the sensor array once every 24 hours by rotating one of the perpendicular sensors and the parallel-mounted sensor 90 degrees around the axis of the remaining sensor; this achieves the same effect, for calibration purposes, as flipping the spin-axis sensor 180 degrees.

The device has a dynamic range of 64 gammas and an individual sensor sensitivity and quantization error (when used with a specially designed 8-bit analog-to-digital conversion unit) of $\pm 1/4$ gamma.

Besides measuring the interplanetary and lunar magnetic fields, this experiment will provide information on the interaction of the solar plasma stream with any lunar magnetic field.

Micrometeorite Flux Experiment (Temple/GSFC)

The micrometeorite (cosmic dust) experiment will measure the momentum, kinetic energy, and velocity of individual dust particles and approximate their radiants. This information will aid in calculating:

- Perturbations of the dust-particle distribution in cislunar space
- Distribution and source (moon or deep space) of dust particles in the vicinity of the moon
- Dust particles associated with meteor streams (both known streams and streams not detectable with ground-based equipment)
- The nature of dust-particle mass distribution in interplanetary space
- The effects of the geomagnetic wake tail and on dust-particle distribution and direction at lunar distances.

The micrometeorite experiment, consisting of two independent detectors, one directional, one nondirectional, is designed to measure dust-particle velocities from 1.5 to 50 km per second and masses from 10^{-13} to 10^{-9} gram. The nondirectional detector is a 312-cm^2 impact plate deposited with a thin film capacitor (ionization sensor) and an acoustic transducer. The kinetic energy of a dust particle impacting on this plate causes the particle to evaporate into an ionized gas; this ionized gas, in conjunction with the thin film capacitor, produces an electrical pulse that can be related to the kinetic energy of the particle. The mechanical energy imparted to the plate by particle impact actuates the

acoustical transducer, producing an output pulse related, by pulse height, to the momentum of the particle.

The directional detector is a tube with a thin film capacitor covering the aperture and an impact plate deposited with a thin film capacitor at the base. An acoustical transducer is attached to the impact plate. The sensor, mounted near the nondirectional detector impact plate with its longitudinal axis perpendicular to the impact plate, monitors in the same manner as the nondirectional detector. The arrangement of the two detectors allows determination of the direction and the speed of particles impacting on both.

Solar-Cell Damage Experiment

The solar-cell damage experiment is a GSFC engineering experiment which will provide information on radiation damage to solar cells and solar-cell cover glass of varying thicknesses and compositions, as well as on the protection afforded solar cells by each type of cover glass.

To accomplish this, one facet of the spacecraft will carry a panel of four groups of sixteen 1-cm x 2-cm n-on-p silicon solar cells with a nominal base resistivity of 10 ohms/cm. Mounting the panel on one of the facets permits cell exposure that will provide meaningful data on most spin-axis/sun line orientations. One group of cells will be unshielded; the second will have an integral 25-micron cover glass; the third, a 6-mil fused silica cover glass; and the fourth, a 6-mil micro-sheet cover.

The sixteen solar cells composing a group are series-connected to a 60-ohm precision resistor of the size required to produce a 4.0- to 4.5-volt output under space conditions with normal illumination. These solar cells are typical production cells or a type which have undergone extensive laboratory testing to determine electron and proton effects. Therefore, output variations among solar-cell groups can be related to solar-cell or solar-cell cover-glass damage. A thermistor imbedded in the solar-cell panel just under the solar cells will monitor variations in experiment temperature.

To assure experiment accuracy, the cell groups will be calibrated for illumination, angle of incidence, and temperature effect, both after environmental testing and before flight.

Passive Experiments

The passive experiments will use the telemetry and the range and range-rate signals as data sources to study selenodesy and propagation of lunar ionosphere radiowaves.

A. M. Peterson (Stanford University) will study the spacecraft telemetry signal to determine the effects of the lunar ionosphere on radio-wave propagation.

W. M. Kaula (University of California, Los Angeles) will analyze variations in the range and range-rate tracking data to obtain selenodetic information.

SPACECRAFT AND SUBSYSTEMS

Structure

Figures 4 and 5 show side and top views of the anchored IMP structure, a two-piece magnesium axial-thrust tube with a Delta attach flange on one end and a retromotor flange on the other; an octagonal aluminum-honeycomb equipment deck with eight radial support struts; an aluminum-honeycomb top cover; and four support brackets and arms for solar-cell paddles and two support brackets and booms for the magnetometers. Experiments and electronics are mounted on the periphery of the equipment deck in modular support frames (Figure 6). The top cover encloses all equipment mounted on the deck, provides an RF ground plane, and furnishes exterior surfaces for the passive thermal-control coatings. Four single RF pivoting turnstile antennas screw into cups protruding through the cover.

The Thiokol TE-M-458 retromotor, bolted to an epoxy-fiberglass adapter ring, is cantilevered from the top flange of the thrust tube. The motor case is mounted by a bolt-lug arrangement that accommodates motor-case thermal expansion and provides adjustment for motor/spin-axis alignment. The fluxgate experiments are mounted on extendable booms projecting from the lower surface of the octagonal equipment deck. All structural components will be made from materials of low permeability (less than 1.001) to meet the magnetic cleanliness requirements of the magnetometer experiments.

Table 1 lists the weights of the spacecraft components.

In the launch configuration (Figure 7), the solar array and fluxgate booms are folded and secured in a position along the X-258 third stage. The folded fluxgate booms are located within the area formed by the folded solar array.

The solar array and fluxgate booms are deployed after third-stage burnout, but before third-stage separation (approximately one minute after the spacecraft is injected into the transfer trajectory). After third-stage separation, this configuration will satisfy the requirement that the ratio of the roll moment-of-inertia

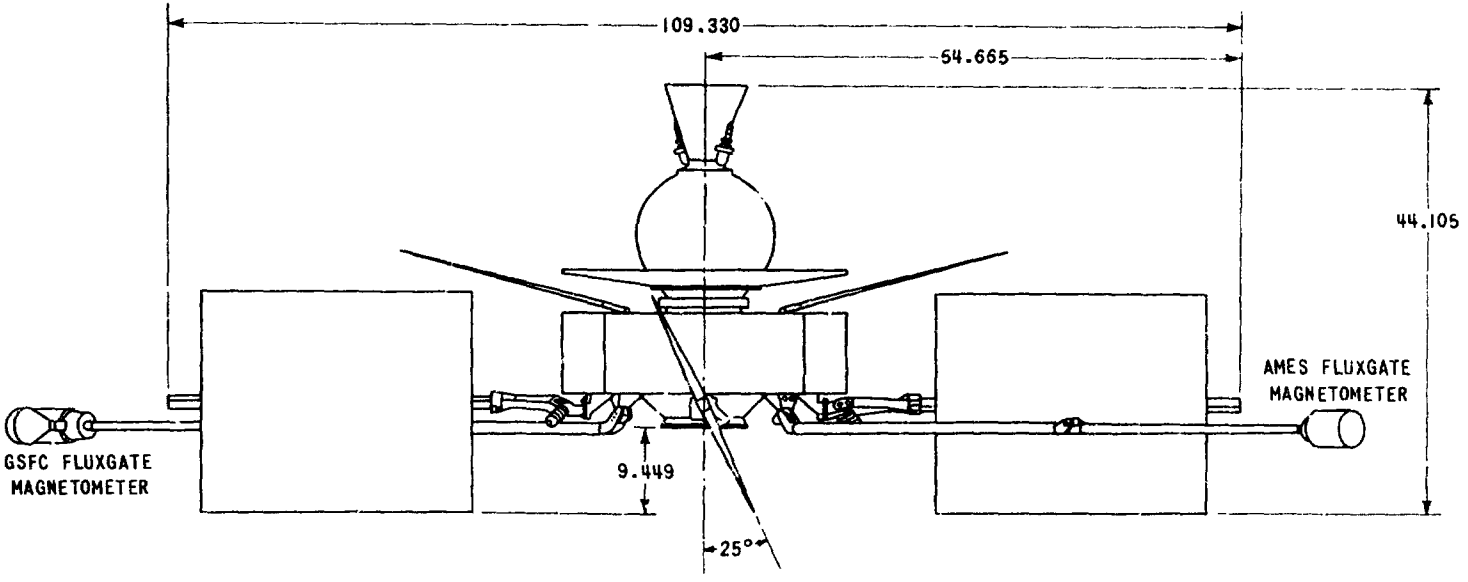

Figure 4. AIMP Spacecraft Side View

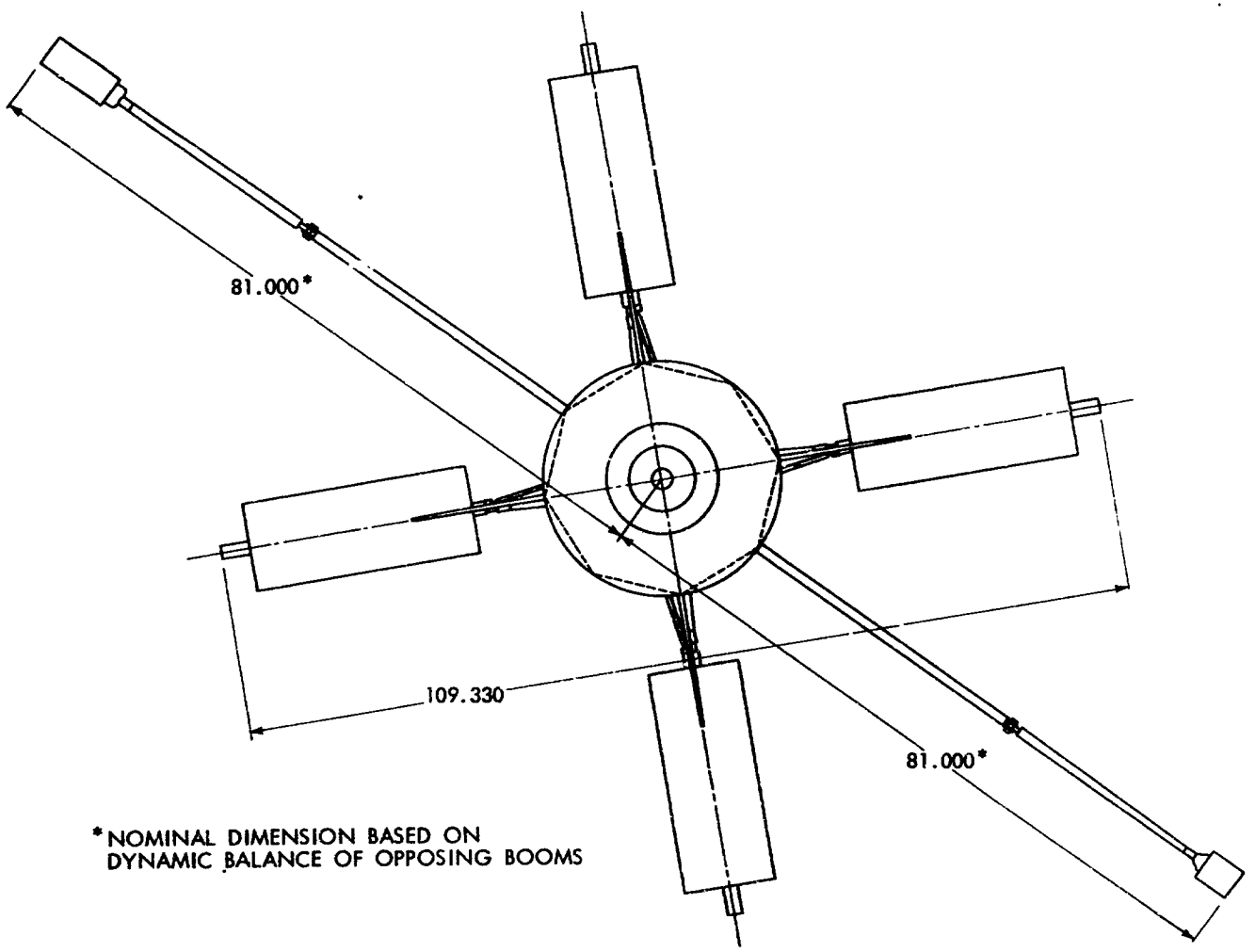

Figure 5. AIMP Spacecraft, Top View

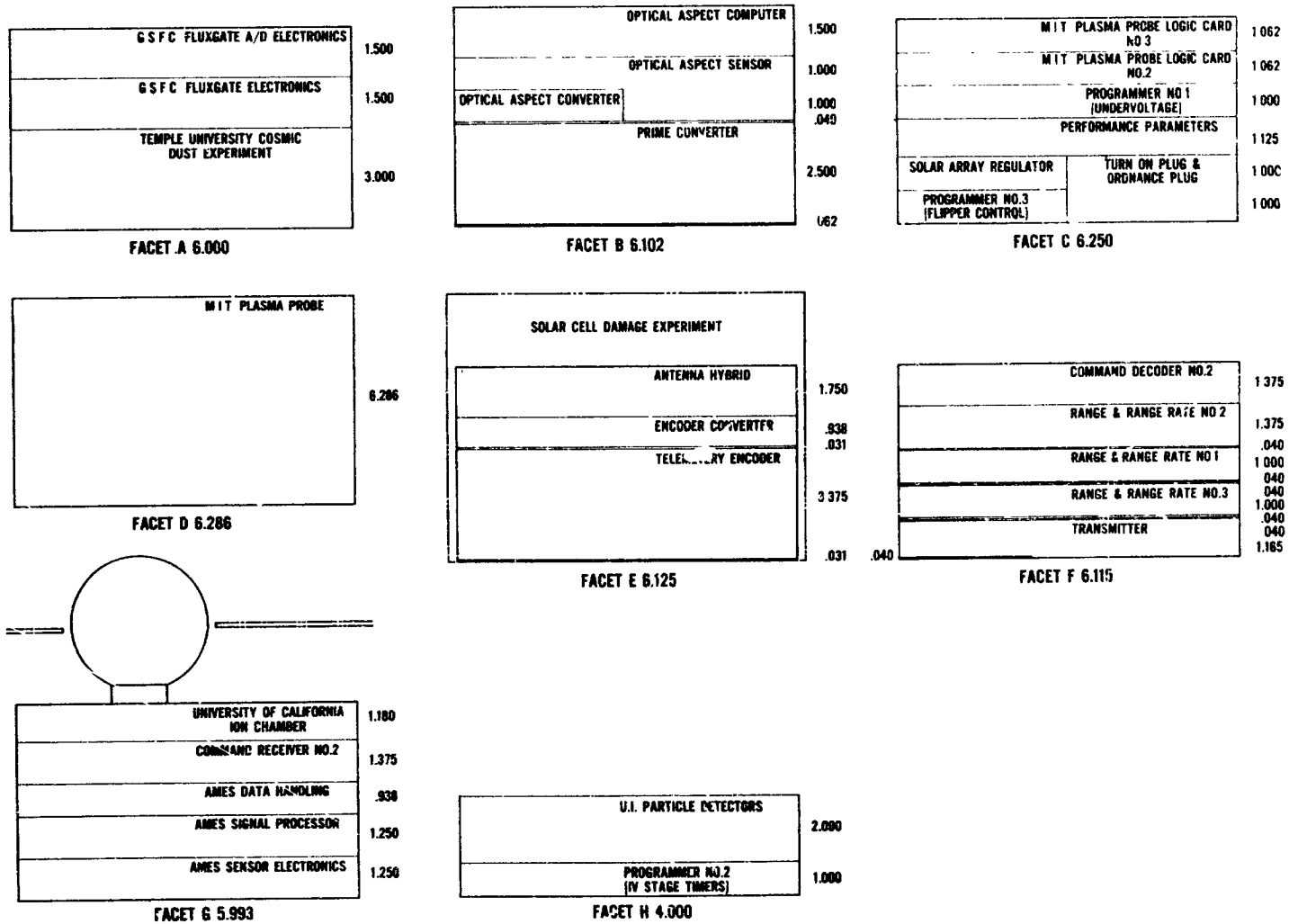

Figure 6. AIMP Modular Frame Locations

Table 1
AIMP-D Weights*

	Weight (lb)
Experiments (21.51 lb subtotal)	
University of California	1.35
Massachusetts Institute of Technology	5.00
State University of Iowa	2.34
Goddard Magnetometer	4.30
Temple University	4.00
Ames Magnetometer	4.30
Solar Cell Experiment	0.22
Telemetry Data System (9.0 lb)	
Programmer #3 (Undervoltage Converter and Detector)	1.00
Programmer #1 (Fourth-Stage Timer)	1.20
Programmer #2 (F/G Flipper Control/Fourth-Stage Parameter)	0.80
Performance Parameters	1.00
Encoder and DDP's	5.00
Telemetry Communications (9.20 lb)	
Transmitter	1.50
Range and Range-Rate #1, #2, #3	4.00
Decoder #2 and Command Receiver #2	2.50
Antennas (Four) and Antennas Hybrid	1.20
Power System (47.70 lb)	
Solar Paddles (Four)	24.60
Battery (YS-10)	10.90
Prime Converter	4.00
Encoder Converter	0.80
Solar Array Regulator	0.40
Internal Electrical	7.00
Optical Aspect System (Sensor, Computer and Converter)	1.75
Structure and Despin Hardware	30.00
Fourth-Stage Motor with Attach Hardware	82.34
X-258 Attach Hardware	4.00
Total Spacecraft Weight	205.50

*Only the structure and incidental hardware have been weighed. The other values are estimates which in some cases appear to be optimistic.

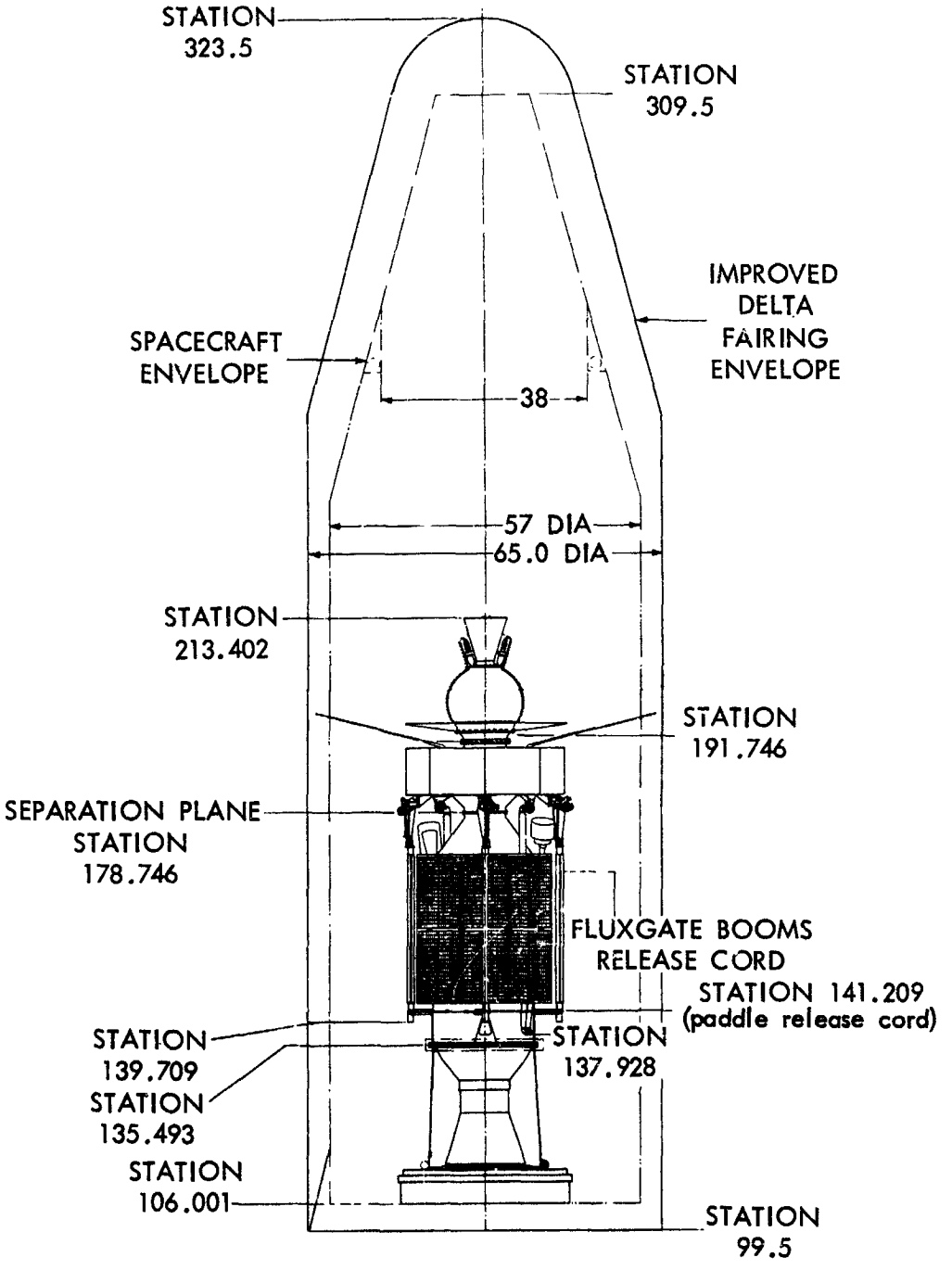

Figure 7. Launch Configuration

to the pitch moment-of-inertia (with the loaded retromotor) will be at least 1.20 during the long coast.

Stabilization

The launch-vehicle guidance system provides stabilization through first- and second-stage burn and the coast-phase pitch program. At the end of the coast-phase pitch program, spin rockets located on a spin-table connection between the second and third stage will spin the spacecraft/third-stage package to a nominal 150 rpm. The expended second-stage motor is jettisoned after spin-up. After third-stage burnout, a yo-yo despin mechanism will reduce the spin rate to approximately 100 rpm. Erection of the solar paddles and the fluxgate booms will further reduce the spin rate to 27 rpm ± 2 rpm. After spacecraft/third-stage separation, the spacecraft-retromotor combination will have roll/pitch moment-of-inertia ratio compatible with the spin rate for adequate spin-stabilization for the transfer trajectory coast period. A yaw or pitch rocket-tumble system will tumble the X-258 to reduce the possibility of spacecraft/vehicle collision after third-stage separation.

At the end of the transfer period, the retromotor will be fired either by direct command or by initiating the onboard fourth-stage timer by ground station command. After retromotor burnout and separation, the spacecraft will have an even more favorable moment-of-inertia ratio for maintaining orbital stability.

To meet these requirements, the combined third-stage/retromotor/spacecraft will be spin-balanced at the Eastern Test Range. The spacecraft and the retromotor will be individually balanced both statically and dynamically before assembly with each other and with the third-stage motor.

Table 2 lists the moments of inertia.

Table 2
Moments of Inertia

Iroll (appendages folded)	3.4 slug ft^2
Ipitch (appendages folded)	6.0 slug ft^2
Ir/Ip (appendages extended during fourth-stage burn)	1.13
Iroll (orbital)	15.2 slug ft^2
Ipitch (orbital)	9.8 slug ft^2
Ir/Ip (orbital)	1.54

Retromotor

The retromotor (Figure 8), a Thiokol Chemical Company TE-M-458 solid-fuel motor using an ammonium perchlorate polyurethane composite propellant, will be used to slow the spacecraft to a velocity that will permit it to be captured in the lunar gravitational field.

The spherical retromotor case, fabricated from titanium (6 AL-4V), is afforded thermal protection by a vitreous silica-phenolic lining and a high-density graphite material throat insert. An asbestos-filled polyisoprene rubber insulator containing an integral separation boot is used to relieve thermally induced strain on the propellant grain. The retromotor case, including the igniters and nozzle, will be insulated to maintain allowable temperatures during the transfer-trajectory period. The retromotor has a burn time of approximately 20 seconds. Spacecraft/retromotor separation is accomplished by an explosive bolt device actuated by ground command, or automatically by the fourth-stage timer 2 hours after ignition.

Thermal Control

Thermal control is achieved through a passive system of surface coatings, insulation, and structural conduction-path design which will maintain temperature gradients and excursions within acceptable limits at the selected solar aspect angles and orbital conditions.

Selection of a transfer trajectory launch window which restricts the solar-aspect angle of the spacecraft/retromotor package to an angle between 30 degrees and 150 degrees, combined with the absorptivity/emissivity ratio of the spacecraft, will keep the spacecraft at suitable temperatures. A thermal blanket of superinsulation will keep the retromotor propellant and retromotor igniters within allowable limits (between 20° F and 140° F) during the transfer-trajectory phase.

During the illuminated portion of the lunar orbit (after retromotor separation), maximum component temperature should not exceed 50° C; minimum temperatures should not fall below -15° C. For shadow periods of 1 hour or less (without power lockout), facet temperatures should not fall below -20° C; however, for longer shadow periods (up to 2.7 hours), facet temperatures in the worst case (when the spacecraft enters the shadow at a solar aspect angle of 180 degrees) can drop as low as -35 to -45° C.

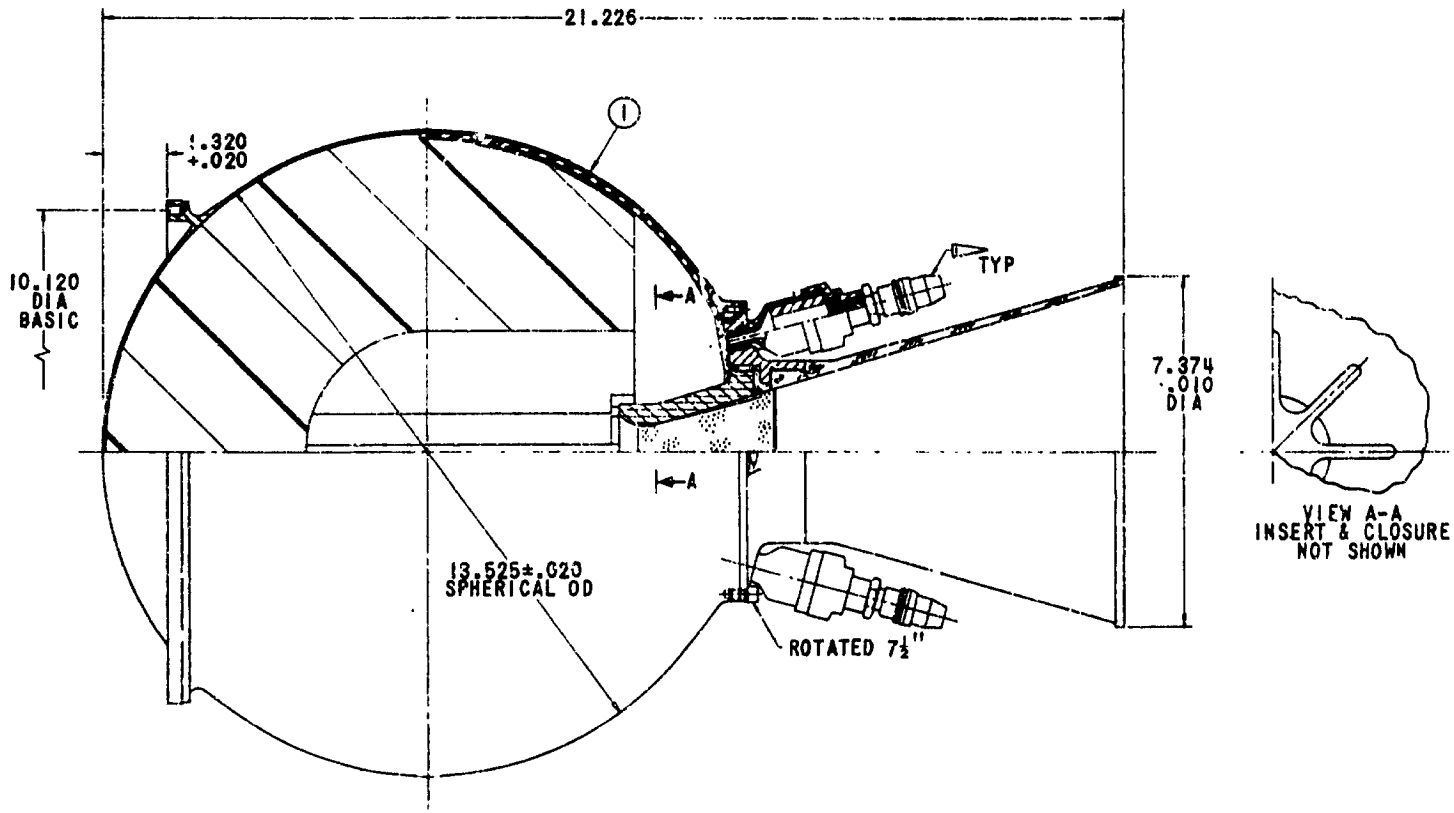

Figure 8. Retromotor

Telemetry Data System

Telemetry Encoder—The telemetry encoder processes data from the various experiment sensors and spacecraft performance sensors (both analog and digital). The encoder design is a unique compromise between weight, size, and power that provides the required data-handling capabilities within the limitations prescribed by spacecraft and launch constraints.

The encoder consists primarily of a voltage-controlled oscillator, a 17-level frequency synthesizer, six 32-bit accumulators, and the spacecraft clock. The voltage-controlled oscillator converts the analog data and the frequency synthesizer converts the digital data to a frequency. Four of the 32-bit accumulators accommodate the University of Iowa electron and proton experiment data; the other two are used in the University of California energetic-particle flux experiment. A simple parity check of the optical aspect data is performed by counting video pulses. The spacecraft clock and binary frequency division provide the required timing signals and sync pulses. Encoder temperature and analog oscillator calibration is monitored and subcommutated in two words of the system performance parameters. Onboard oscillator calibration is accomplished by use of a standard reference voltage (zener standard reference source) and by use of precision wire-wound resistor voltage dividers to produce 4 related calibration voltages.

The encoder system provides for continuous transmission of data (burst-burst) at an average bit rate of 28.5 bits per second (25 bits per second for digital data, 40 bits per second for analog data). Figure 9 shows the encoder format, composed of 10 frames of 16 channels (32 subchannels). Table 3 gives AIMP (IMP-D) frame-sequence assignments for analog performance parameters, and subchannel and bit assignments for digital performance parameters.

Performance Parameters—The spacecraft performance-parameters package includes the circuitry necessary to convert the outputs of the various spacecraft temperature, voltage, and current sensors to inputs acceptable to the analog-to-digital converte of the encoder. The performance-parameters package also contains the 7-volt power source for the temperature transducers, and controls the dumping point voltage of the solar array regulator.

Telemetry Communications System

The spacecraft communications system provides radio links for receiving range and range-rate and ground-command signals, and for transmitting telemetry or tracking data from the spacecraft. The system consists of a telemetry transmitter, a range and range-rate transponder, a redundant command receiver/command decoder unit, and an antenna and hybrid system.

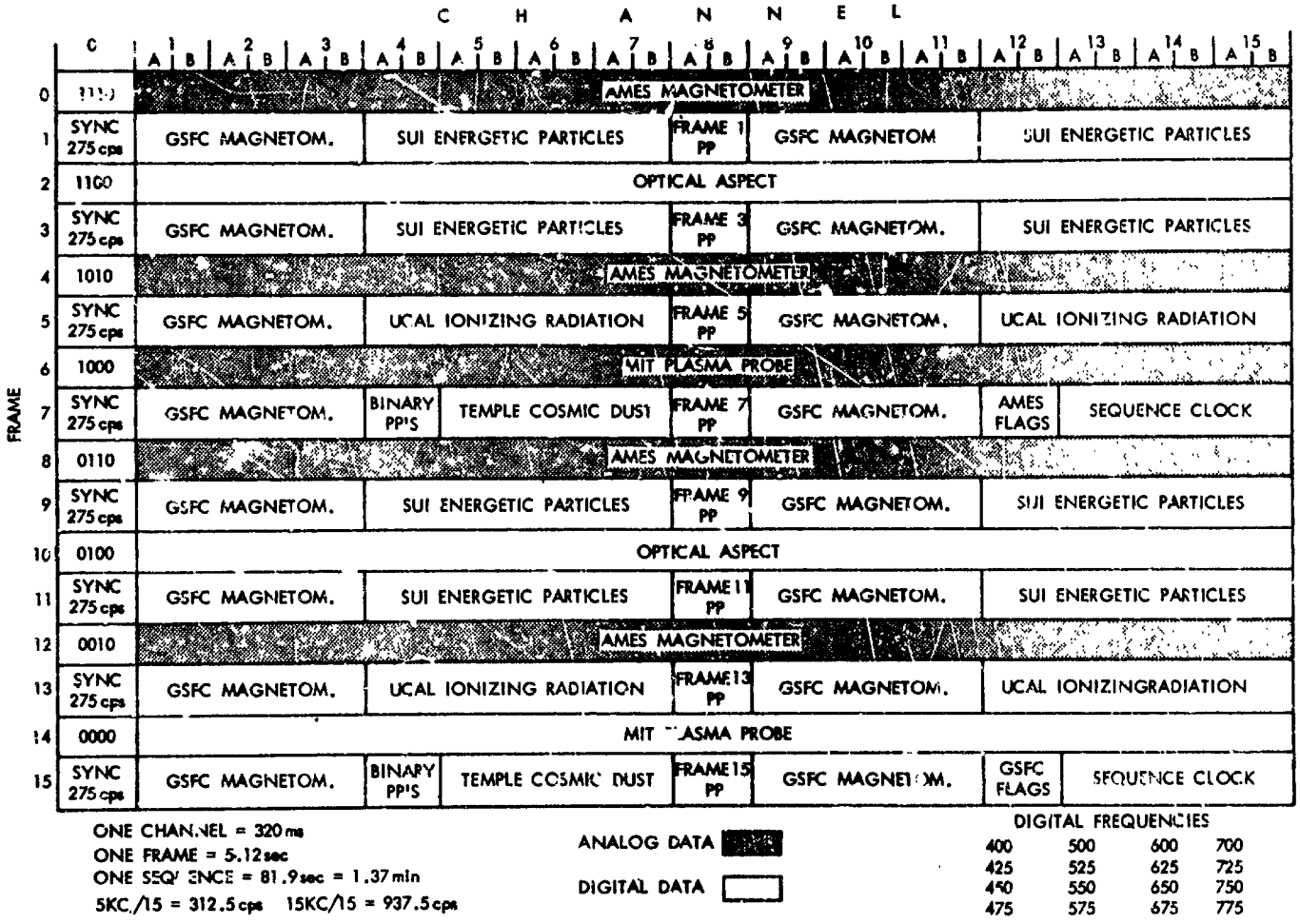

Figure 9. AIMP Encoder Format

Table 3
AIMP-D Performance Parameter Assignments

Channel 8 (8 bits each) - analog input			
Frame No.	Sequence 1	Frame No.	Sequence 3
1	PP1, +12 volts main buss	1	PP1, +12 volts main buss
3	PP2, battery voltage	3	PP2, battery voltage
5	PP3, battery current	5	PP3, battery current
7	PP4, solar-array current	7	PP4, solar-array current
9	PP5, spacecraft current	9	PP5, spacecraft current
11	PP6, +28 volts transmitter	11	PP17, transmitter temperature
13	PP7, +7 volts temperature PP's	13	PP18, battery temperature
15	PP8, UI voltage	15	PP19, prime converter temperature
	Sequence 2		Sequence 4
1	PP9, solar experiment 1	1	PP20, solar-array temperature
3	PP10, solar experiment 2	3	PP21, Ames temperature 1
5	PP11, solar experiment 3	5	PP22, Ames temperature 2
7	PP12, solar experiment 4	7	PP23, GSFC magnetometer temperature
9	PP13, solar experiment temperature		
11	PP14, fourth-stage bottle temperature/ Temple temperature	9	PP24, UCAL temperature
		11	PP25, MIT temperature
13	PP15, fourth-stage bottle temperature/ fourth-stage firing duration	13	PP26, UI temperature
15	PP16, encoder-oscillator calibration	15	PP16, encoder-oscillator calibration
Bit	Channel 4A	Bit	Channel 4B
2^0	BP1, fourth-stage timer #1 first decade	2^0	BP5, fourth-stage timer #2, first decade
2^1	BP2, fourth-stage timer #1, second decade	2^1	BP6, fourth-stage timer #2, second decade
2^2	BP3, third-stage separation/fourth-stage separation	2^2	BP7, magnetometer booms erection
2^3	BP4, separation armed	2^3	BP8, separation armed

Transmitter—The transmitter functions as a 136.020-Mc 6-watt pulsed-frequency-modulation/pulse-modulation (PFM/PM) system with a signal compatible with the STADAN phase-lock receiving systems. The transmitter accommodates both the output of the telemetry encoder and the output of the range and range-rate transponder on a time-sharing basis.

Range and Range-Rate Transponder—The range and range-rate transponder operates in conjunction with the spacecraft transmitter and one of the command receivers to provide ranging data. Either the tone-ranging or the hybrid ambiguity-resolving ranging system, or both, can be used. The range data information transmitted from the spacecraft will be centered around a sideband 905 kc from the 136.020-Mc carrier.

Command Receivers and Decoders—The command system includes two command receivers and two command decoders. The command system will use a frequency of 148 Mc transmitted by the 10-kw transmission/reception VHF antenna system of the range and range-rate system. The signal will be received by the turnstile telemetry antenna (zero db gain) on the spacecraft and fed to the redundant command receivers which have a sensitivity of -118 dbm.

The command sequence will consist of an address tone followed by three execute tones (ACCC). The following is a list of commands to be available on the AIMP:

1. Start fourth-stage timers (two-hour timers)
2. Stop fourth-stage timers
3. Direct fire fourth stage (interlocked with command No. 1)
4. Arm separation (interlocked with command No. 1)
5. Direct separation (interlocked with command No. 1 and 4)
6. Transmitter ON
7. Transmitter OFF
8. Initiate undervoltage cycle (locked out until fourth-stage separation)
9. Range and range rate reset
10. Range and range rate ON

To direct fire the fourth stage, commands No. 1 and 3 must be given in sequence, but not necessarily at the same time. To direct separate, commands 1, 4, and 5 must be given in sequence but not necessarily at the same time. Command 2 stops the timers and resets command 4 to the OFF position. Command 10 is not a normal command since it operates off the receipt of an address tone and the 4-kc range and range-rate tone. The system is locked in the range and range-rate mode as long as the 4-kc tone is present (a fast detect slow decay circuit is used so the system does not drop out of range and range rate due to antenna nulls).

Antenna and Hybrid—The spacecraft antenna system consists of four dipole antennas spaced 90 degrees apart on the upper surface of the octagonal cover and elevated at an angle of 15 degrees from the attaching point to form a canted turnstile. The antennas are fed in phase quadrature to produce a standard IEEE radiation pattern; i.e., left-hand circularly polarized from the top, linearly polarized from near the center, and right-hand circularly polarized from the bottom. The antennas are fed from a 90-degree stripline coupler/duplexer.

The transmitter and one command receiver are connected to the antenna through the duplexer; the second command receiver through a separate coupler. Transmitter output is fed through the coupler to opposing antenna pairs connected by a half-wavelength cable. The signals to each pair are equal in power but 90 degrees out of phase.

Power System

Solar Array—Conversion of solar energy by 7680 2 x 2 cm silicon cells, located on four 25.25-inch-wide by 27.6-inch-long paddles extending on arms from the equipment deck, provides power to the AIMP. The paddles are oriented to allow a near-uniform solar-cell projection area at any spacecraft solar attitude. The solar-cell requirement was established by considering the variation in spacecraft and experiment power demands during light and shadow periods, and by a statistical analysis of probable cell failure. The cells are connected in series-parallel arrangements based on the probable-failure mode of the cells in conjunction with the voltage-current requirements of the spacecraft. Table 4 shows solar-array power output.

Solar Array Regulator—The solar array regulator functions to prevent excessive voltage generated by the solar cells from damaging the spacecraft and its battery. The regulator will operate in either of 2 stable states depending upon the state of charge of the battery. A current sensor in the battery charge circuit determines the state of charge. When the battery requires charge currents in excess of 100 ma, an appropriate signal to the regulator will set the

regulation at 19.6 volts. When the battery charge current diminishes to less than 50 ma, the regulation will be at 18.3 volts, the purpose being to eliminate the possibility of cell unbalance such as would occur at the higher potential.

Table 4
Solar-Array Power Output
(watts)

	Normal Operation (19.6 v)		Shadow Emergence (15.5 v)	
	Average Minimum (rotation)	Instantaneous Minimum	Average Minimum (rotation)	Instantaneous Minimum
Initial	66.1	54.4	57.9	47.6
End of life	56.2	46.3	49.2	40.5

Battery—The storage battery is a sealed nonmagnetic silver cadmium battery, rated at 11 ampere-hours. It is composed of 13 cells in series, which provides a battery discharge voltage, when fully charged, of 15 volts (1.15 volts/cell) and 12 volts (0.93 volts/cell) when fully discharged. Discharge below the 12 volts is detrimental to the battery and accordingly an undervoltage relay is used to disconnect the loads from the system below this value. The maximum safe charge voltage is 19.6 volts. This allowable safe limit is maintained by a battery charge regulator which operates by shunting the solar array output. Continuous charging at 19.6 volts, after the battery is fully charged (battery accepts less than 100 ma of current), is considered detrimental to the battery and therefore the regulator is designed to reduce the charge voltage to 18.3 volts upon full charge of the battery. This reducing charge current to a trickle rate.

Prime Converter—All major experiments and instruments power will be supplied from the prime converter; only control systems such as the undervoltage and solar-array regulator will operate directly from solar array or battery power. The prime converter will provide three regulated voltages under the load conditions specified in Table 5.

Table 6 shows the power allotment for the various experiments and systems.

Table 5
Converter Characteristics

Voltage	Regulation (1%)	Load (Milliamperes)			Minimum Short Circuit Capability
		Min.	Avg.	Peak	
12	±1	600	620	650	200% (of largest fuse rating)
20	±1	80	100	260	200% (of largest fuse rating)
28	±1	590	590	590	None

Optical Aspect Converter—The purpose of the optical aspect (OA) converter is to supply to the OA computer and sensor the specified voltages as indicated in Table 7.

The converter can be operated without a load on any or all outputs although regulation will not be maintained on the unloaded outputs. The converter operates in specified limits with an input voltage of +20 volts ±1 percent.

Encoder Converter—The purpose of the encoder converter is to supply to the encoder the specified voltages as indicated in Table 8.

The converter operates within the specified limits over an ambient temperature range as indicated in Table 7 and can operate without a load on any or all outputs although regulation will not be maintained on the unloaded output.

The converter operates within the specified limits with an input voltage of +12.0 volts ±1 percent.

Programmers

Undervoltage Detector—The undervoltage detector consists of a voltage sensor, 4-hour timer, and appropriate control and switching circuitry. The detector monitors the battery voltage and turns off the prime converter power when the battery voltage drops below 12 ± 1/4 volts. When turned off, the prime converter power remains off until turned on by the 4-hour timer or by the battery voltage returning to 18 volts. If, at the end of the 4-hour period, the battery voltage is not greater than 12 ± 1/4 volts, the undervoltage detector will reset the timer for another 4-hour period. To permit battery charging for periods of 4 hours, regardless of system voltage level, the 18-volt turn-on function is disabled when the undervoltage detector is actuated by ground command.

Table 6
AIMP Power Allotment

	Initial (Nominal) Watts	End of Life (Worse Condition) Watts
Solar Array Output	66.1	49.2
	Peak (Watts)	Average (Watts)
System Voltage (12—19.6) Breakdown		
Undervoltage detector	.240	.240
Solar array regulator	.196	.196
GSFC or Ames magnetometer flipper	4.000	.028
Total	4.436	.464
Regulator Converter Breakdown		
Experiments		
Ames magnetometer (+12v)	.800	.800
GSFC magnetometer (+12v)	1.000	1.000
University of California (+12v)	.200	.200
Temple University (+12v)	.500	.500
University of Iowa	.700	.700
MIT (+20v)	3.500	1.100
Total	6.700	4.300
Telemetry		
Encoder and DDP system (+12v)	2.380	2.150
Transmitter (+28v)	16.500	16.500
Range and range rate and command (+12v)	1.610	1.610
Total	20.490	20.260
Instruments		
Optical aspect system (+20v)	1.500	.950
Performance parameters (+12v)	.137	.137
Fourth-stage electronics (+12v)	.420	.000
Fourth-stage parameter (+12v)	.240	.240
Total	2.297	1.327
Total prime converter load	29.480	25.887
Input to prime converter at 74% efficiency	39.897	34.982
Load on 12—19.6v bus	4.436	.464
Regulator-converter input	39.897	34.982
Battery charging	8.000*	8.000
Total power allotment	52.333**	43.446

*Battery charge not an actual peak demand load-nominal figure only.
**True peak demand load 44.333w.

Table 7
Optical Aspect Converter Output Voltage

Output[1] Voltage	Regulation	Ripple	Load	Temp. Limits (°C)
+12.0 v	± 5.0%[2]	None specified	12 ma	-10 to +60
+ 3.5 v	±10.0%	None specified	143 ma avg. 286 ma peak	-10 to +60

(1) Outputs are not protected against shorts.
(2) The +12-volt line exhibits a source impedance of less than 5 ohms for a step change in load of 1 ma (around the nominal load) from dc to 1 kc. The +12-volt output has a ±5 percent tolerance for changes in nominal voltage due to temperature, drift, and input voltage variation.

Table 8
Encoder Converter Output Voltage

Output[1] Voltage	Regulation	Ripple	Load	Temp. Limits (°C)
- 9.0 v	±10.0%	None specified	0.5 to 1 ma	-30 to +60
- 4.0 v	± 5.0%	None specified	45 to 50 ma	-30 to +60
+ 6.5 v	± 5.0% ± 1.0%	None specified	50 to 70 ma	-30 to +60 0 to 40
- 3.0 v	± 5.0% ± 1.0%	None specified	1 to 11 ma	-30 to +60 0 to +40
7.5 v	± 0.25% ± 1.0%	None specified	1 to 5 ma	0 to +40 -10 to +60

(1) Outputs are not protected against shorts.

Fourth-Stage Timer—The fourth-stage (retromotor) electronics package is a redundant set of 2-hour timers initiating retromotor ignition and retromotor separation (both timers perform both functions), and a direct command ignition and separation circuit. The timers operate on ground command at the appropriate time during the transfer trajectory period.

Flipper Control and Fourth-Stage Burn Timer—The flipper control applies power to each individual magnetometer flipper (sensor rotating device) alternately for a period of 10 minutes every 12 hours. Power lines between the flipper control and each experiment flipper are individually fused to prevent failure of one flipper from interfering with the operation of the other. Control time determination is obtained from the encoder timing pulses; flipper operating power comes directly from the solar array battery combination.

The retromotor performance monitor is a thrust-actuated switch operated by the deceleration caused by retromotor ignition, plus a timing circuit that monitors retromotor burn time. This information, transmitted to the ground as part of the performance-parameter telemetry, will be used with tracking data for calculating total retromotor impulse.

Despin Function—The DAC third-stage sequence timer package will provide the power pulse to the yo-yo despin dimple motors on the spacecraft through a flyaway connector in the third-stage interface.

Optical Aspect

The optical aspect system consists of four sensors and associated electronics. One of the sensors (180-degree field-of-view digital output solar aspect sensor) will be used to determine the angle between the spacecraft's spin-axis and the sun. The sensor is capable of resolving the spin-axis/sun angle within ±0.5 degree.

The remaining three sensors are pencil-beam (0.25-degree field-of-view) telescopes. The three sensors are mounted at angles of 45 degrees, 90 degrees, and 135 degrees to the spin-axis; the sensors, if actuated by reflected light from earth or moon, provide digital outputs, reflecting the angle subtended by the moon or the earth from each sensor angle, and the angle through which the spacecraft rotates between sun-sensing and earth or moon horizon-sensing (centerpoint of the three sensors). In addition, one of the sensors will provide a digitized video signal of an approximately 10-degree portion of its sweep across the moon's (or earth's) surface.

The optical aspect system will furnish a sun pulse or in shadow a pseudo sun pulse to the experiments requiring it.

If the transfer-trajectory injection point occurs when the sunlit earth is observable by the optical aspect telescopes, the telemetered data will help to determine the spacecraft's actual orientation in space. This unambiguous information will also be used as one of the inputs to calculate retromotor firing time. If injection occurs at a time when the earth is in shadow as seen by the OA detectors, the predicted spin-axis/sun angle will be compared with sensor spin-axis/sun angle data to determine the approximate spacecraft orientation.

When the spacecraft is in lunar orbit, sensing the edge of the moon and the associated low-resolution video scan of its surface may make it possible to compute spacecraft spin-axis orientation very accurately.

DECONTAMINATION AND CLEAN-ROOM ASSEMBLY

The AIMP spacecraft will be assembled under conditions that will minimize the possibility of contaminating the lunar surface with earth-originated microorganisms insofar as this can be done without jeopardizing spacecraft or mission reliability. A clean room will be provided at both GSFC and Cape Kennedy for component and spacecraft decontamination and clean assembly. The decontaminated spacecraft will be shipped in a sterile container to ETR, where it will be assembled with mating components in the ETR clean room. Exact procedures to be used at both locations are under study and a more detailed description will be available at the conclusion of these studies.

TING

Objectives of the test program are to determine the ability of the spacecraft and equipment to meet design performance requirements, and to demonstrate system reliability and dependability. All experiments and instrumentation must meet the AIMP Test and Evaluation Specification developed by the Test and Evaluation Division, GSFC.

Before spacecraft assembly, critical spacecraft hardware and all experiments and instruments will undergo a series of operational tests to determine their flight worthiness. Operational and environmental tests of the assembled spacecraft will assure meeting overall system performance requirements.

LAUNCH VEHICLE

The basic launch vehicle will be an improved DSV-3E Delta (Figure 10).

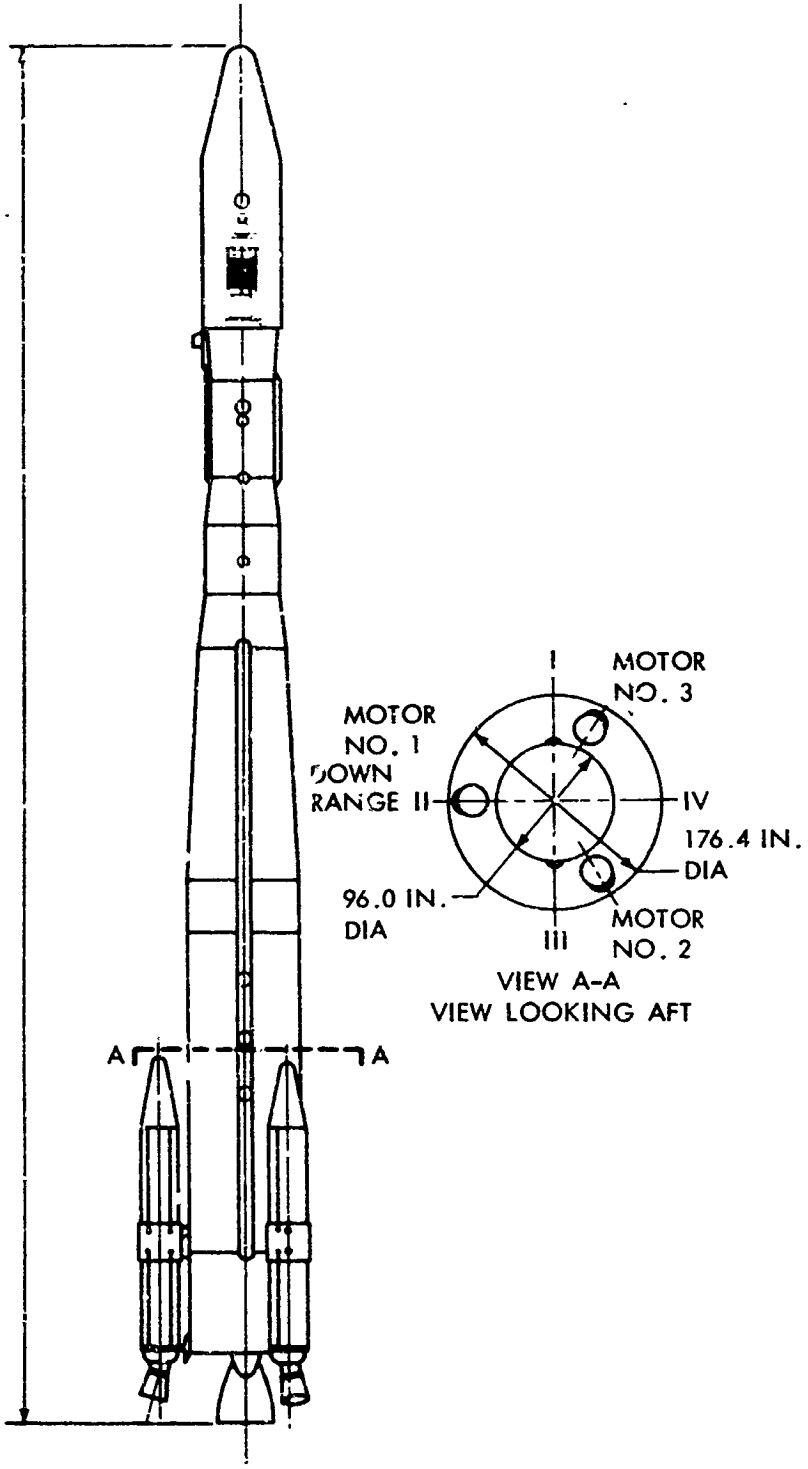

Figure 10. DSV-3E Launch Vehicle Profile

The DSV-3E is a three-stage booster that consists of a DSV-3E-1 first stage, DSV-3E-4 second stage, and an X-258 third stage.

First Stage

The first stage (DSV-3E-1) consists of a DSV-2C booster modified by the addition of three strap-on Thiokol TX-33-52 solid-fuel rocket motors. The DSV-2C is powered by an MB3-Block III, Rocketdyne liquid oxygen (LOX)-RJ-1 rocket motor. The main engine is gimbal-mounted to provide pitch and yaw control from liftoff to main-engine cutoff (MECO). Two 1000-pound-thrust liquid-propellant vernier (XLR-101-NA-11) engines provide roll control throughout first-stage operation and take over pitch and yaw control from MECO to first-stage separation.

Second Stage

The second stage (DSV-3E-4) is an Aerojet General Corporation AJ10-118-E liquid-fuel engine employing inhibited red fuming nitric acid (IRFNA) and unsymmetric dimethylhydrazine (UDMH) as the propellant. The second-stage main engine is also gimbal-mounted to provide pitch and yaw control through second-stage burn. A nitrogen gas system utilizing six fixed nozzles provides a roll control during powered flight and coast flight, and a yaw control after second-stage cutoff (SECO). The second stage also has two fixed-nozzle deceleration and tumble motors to prevent a collision after second-stage separation. The motors are fed from the propellant-tank helium pressurization supply.

Third Stage

The third stage is a spin-stabilized solid-propellant ABL-X258-E2 rocket having a payload-attach structure fixed to the forward-engine adapter ring and containing a spring for third-stage separation. A Nimbus type shroud attached to the second stage protects the third stage and spacecraft during flight through the atmosphere. The second-to-third stage connection is a spin table and petal arrangement fixed to the second stage, and a band containing explosive bolts which hold the third stage on the petals. A set of rockets fixed to the spin table provides spin-up.

Guidance and Control

Preprogrammed autopilots control the vehicle (DSV-3E) and the sequence of operations from liftoff to second-stage separation. The second-stage autopilot can supply five discrete steering commands, and six flight-sequence signals. Between second-stage ignition and separation, up to three pitch rates and

two yaw rates can be obtained by the five steering commands. Because third-stage attitude is determined from second-stage pitch and yaw rates during the coast period, the coast phase rates are limited to 0.1 to 1.0 degree per second. Command rate control can be initiated several seconds after SECO and continues to within 25 seconds or less of third-stage separation. The time interval—the time required to damp out transients—will be 25 seconds for the 1.0 degree per second rate and less as the rate decreases. The rates will be kept as low as possible to conserve control gas.

A BTL radio-command guidance system is used to correct trajectory error from about 90 seconds after liftoff until the lower limit of the tracking radar is reached. When ground guidance is terminated, an integrating accelerometer is actuated to command SECO.

MISSION PLANNING

The Space Science and Satellite Applications Directorate and the Tracking and Data Systems Directorate share the responsibility for mission planning and analysis and for data processing. Field station operations are initiated and coordinated through the Project Operations Support Division of the Tracking and Data Systems Directorate.

The Systems Analysis Office and the Delta office will prepare launch windows for launch opportunities calculated from the combined preliminary findings of both offices. Figure 11, prepared from data furnished by the Systems Analysis Office, illustrates a typical lunar insertion window but does not include the limitation in insertion time arising from lifetime and shadow restraints. Figure 12 gives two possible variations of this typical trajectory which were produced during a Monte Carlo study using the vector of injection into the transfer trajectory associated with the curves in Figure 11, and the 1σ error associated with the injection vector.

The Delta office has determined that the launch window for the Delta vehicle will be 3 minutes a day, and that a different launch azimuth will be used on each of the 4 to 5 consecutive days of a lunar month when a launch opportunity exists. Studies by both the Systems Analysis Office and the Delta Projects Office have shown that launch opportunities exist in 2 consecutive lunar months twice a year.

Figure 13 shows beginning, middle, and end subsatellite plots of nominal transfer trajectories for the 1966 launch opportunity.

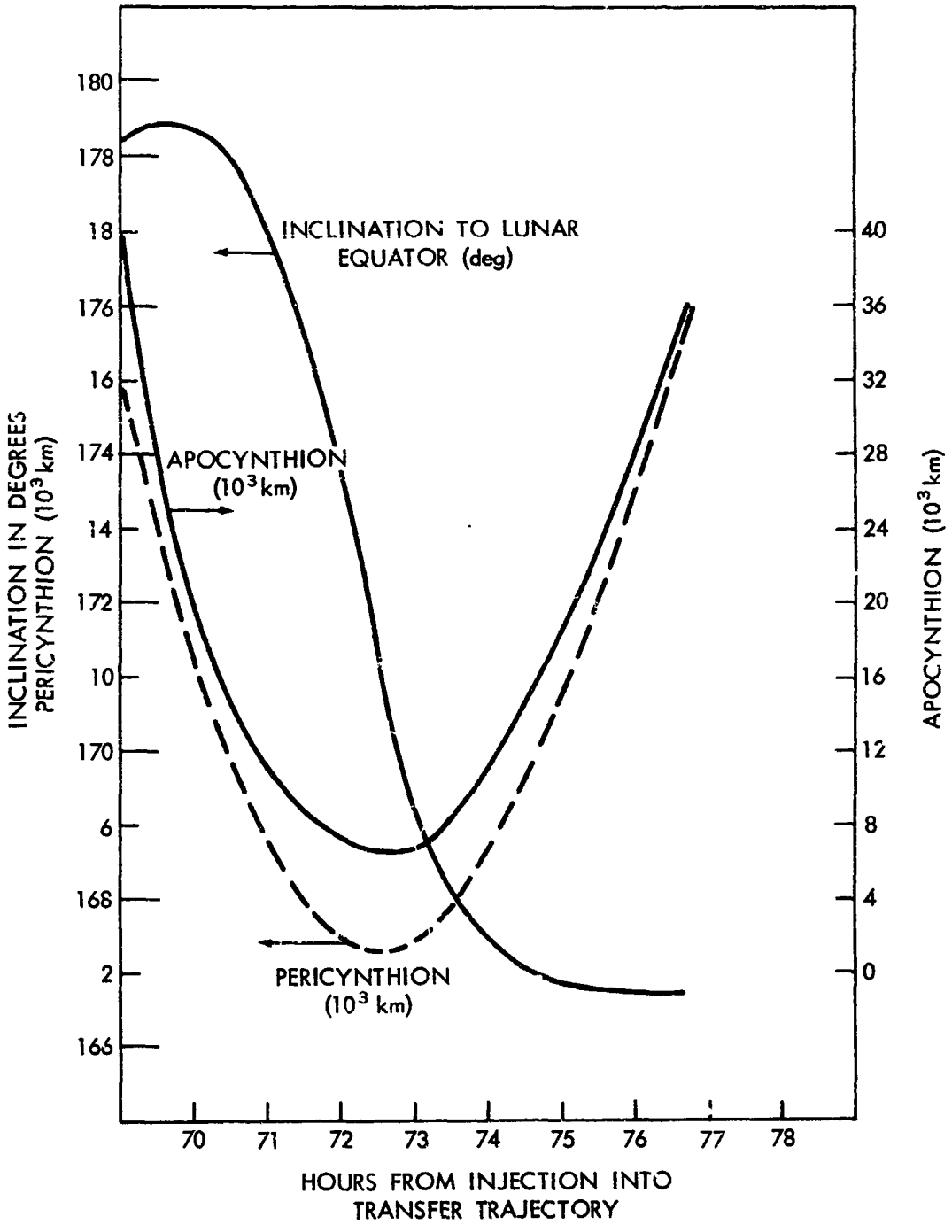

Figure 11. Typical Nominal Lunar Insertion Window

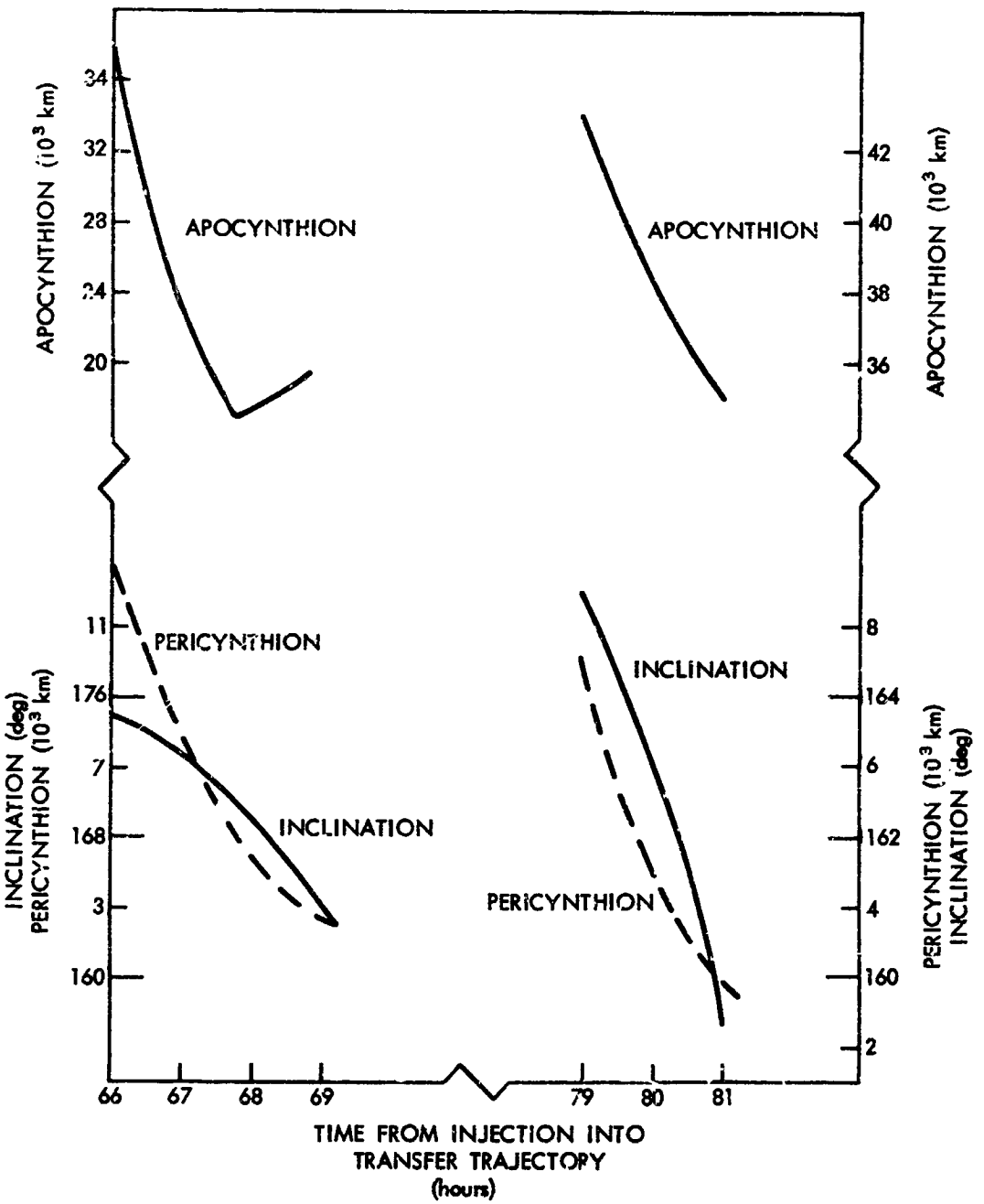

Figure 12. Variations of Insertion Window

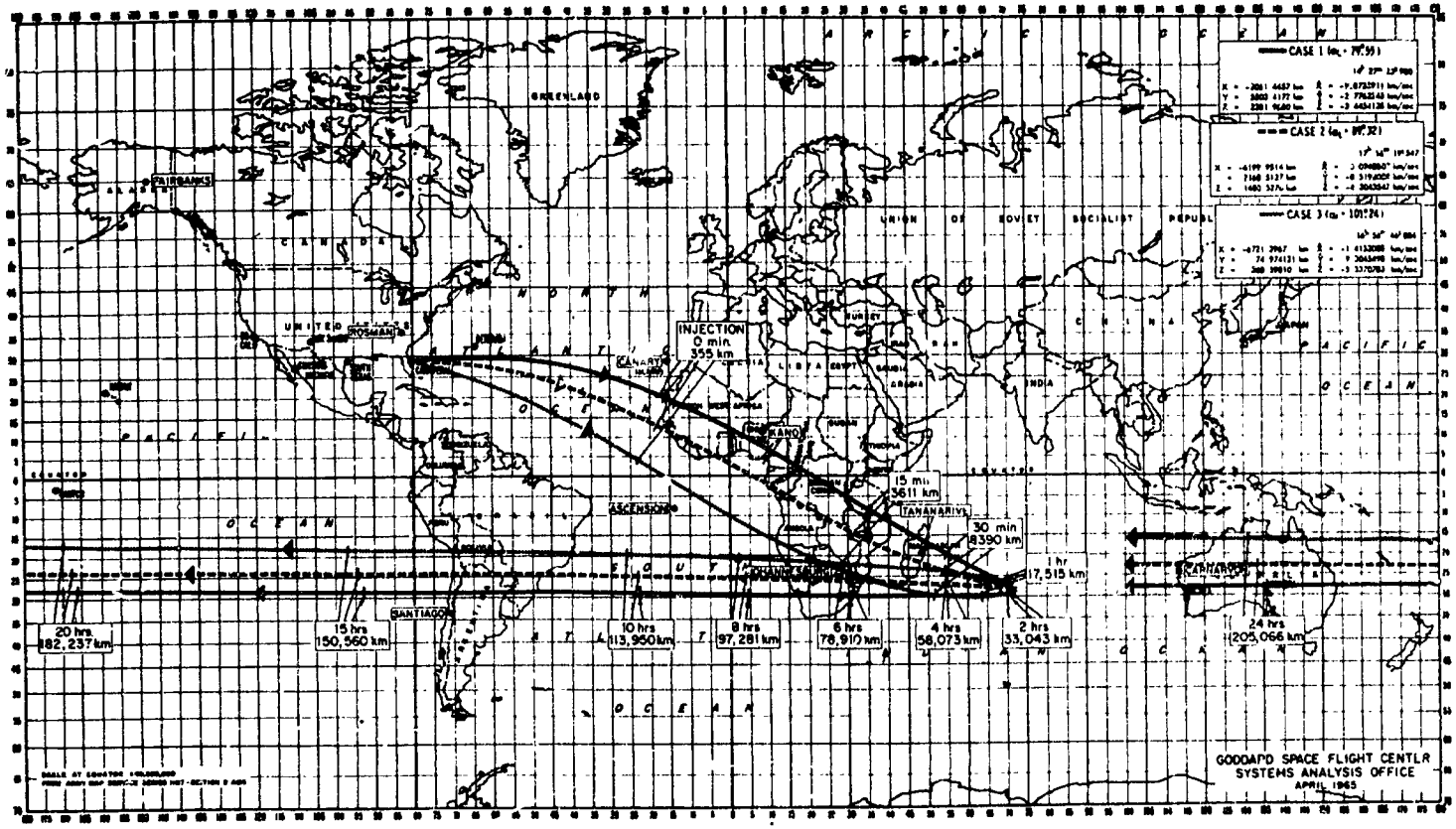

Figure 13. Nominal Transfer Trajectory Subsatellite Plots

ORBIT AND TRAJECTORY

Figure 1 shows a typical sequence of events for launching an AIMP into lunar orbit using the improved Delta (DSV-3E) launch vehicle. The range of acceptable lunar orbital parameters is:

- Inclination — 140 to 180 degrees
- Pericynthion — 500 km
- Apocynthion — Lowest possible

Trajectory requirements are:

- Launch azimuth — 75 to 100 degrees
- Injection velocity — 35,000 feet-per-second
- Liftoff to third-stage separation — 1222 seconds
- Flight time to moon — Approximately 5 hours

The launch azimuth will vary from day to day but will remain constant during each daily 3-minute launch window. Injection velocity for each launch azimuth will vary slightly (a few feet per second); however, the lift-off to injection time will remain constant.

TRACKING OPERATIONS AND CONTROL CENTER

Tracking Operations

The AIMP will be tracked primarily by the STADAN stations equipped with the GSFC range and range-rate system.

At launch, the tracking will be done by the ETR tracking network assisted by the applicable STADAN and MSFN stations. The launch tracking data plus the nominal second- and third-stage performance information, will be used to generate the initial transfer-trajectory parameters.

The Manned Flight Operations Division, using the above data and the output of the STADAN range and range-rate and Minitrack systems will generate the

transfer trajectory parameters and a set of curves showing the lunar orbital parameters attainable for different fourth-stage firing times.

Ranging System Power Calculations

Table 9 gives the power calculation for the most recent GSFC range and range-rate ground equipment. The older equipment has similar capabilities.

Control Center

An AIMP Control Center, located at GSFC, will monitor the AIMP spacecraft status, will direct the commands to be transmitted by the AIMP Range and Range Rate stations during the lunar transfer trajectory and will be activated if the spacecraft develops problems when it is in the lunar orbit.

Figure 14 shows the data flow from the field station to the control center; the data alarm indicated in this diagram is a special computer printout that occurs when the spacecraft is in a premature fourth-stage operation mode.

Only spacecraft-status information (performance parameters) and optical aspect data will be transmitted in near real time from the field stations. No experimenter data will be processed by this system. The manual back-up data processing at the station will be transmitted by voice link or teletype.

GROUND SYSTEMS

Launch Vehicle Ground Support Equipment

The Eastern Test Range, the launch vehicle contractor (Douglas Aircraft Company), and the retromotor contractor (Thiokol Chemical Corporation) will supply suitable personnel and equipment to handle the following tasks:

- Assemble the Delta launch vehicle
- Assume responsibility for checkout of the vehicle's transmitters and range safety beacon
- Install and arm retromotor
- Prelaunch checkout and launch of the vehicle

GSFC will be responsible for delivering the completed AIMP (D&E) spacecraft to ETR and for an operational checkout of the spacecraft after it is

Table 9

VHF Performance Summary

AIMP PREDICTED PERFORMANCE OF ALASKA AND SANTIAGO R&RR SPACECRAFT RANGE (KILOMETERS) 4000,000 KM

P_T	= 6 watts	= + 37.8 DBM
G_T	=	= - 4.0 DBM
A_T	=	= -188.0 DBM
G_{GR}	=	= + 21.0 DBM
ANOMALIES	=	= - 6.0 DBM
S	=	= -139.2 DBM ASSUME -140 DBM
Φ	=	= -167.9 DBM/CPS
S_T/Φ	=	= + 28.7 DBM/CP

CARRIER LOOP S/N (10 CPS $2B_L$) = +11.3 DB

SUBCARRIER LOOP S/N (10 CPS $2B_L$) = +10.0 DB

20 KC TONE S/N (0.1 CPS $2B_L$) = +27.0 DB

PREDICTED RANGE ACCURACY = 45 METERS RMS

PREDICTED RANGE RATE ACCURACY = 0.2 METERS/SEC. RMS

ASSUMPTIONS:
1. Parallel Ranging Model
2. Narrowest Bandwidths Used
3. 20 KC is highest ranging tone
4. Data rate is 1/sec.

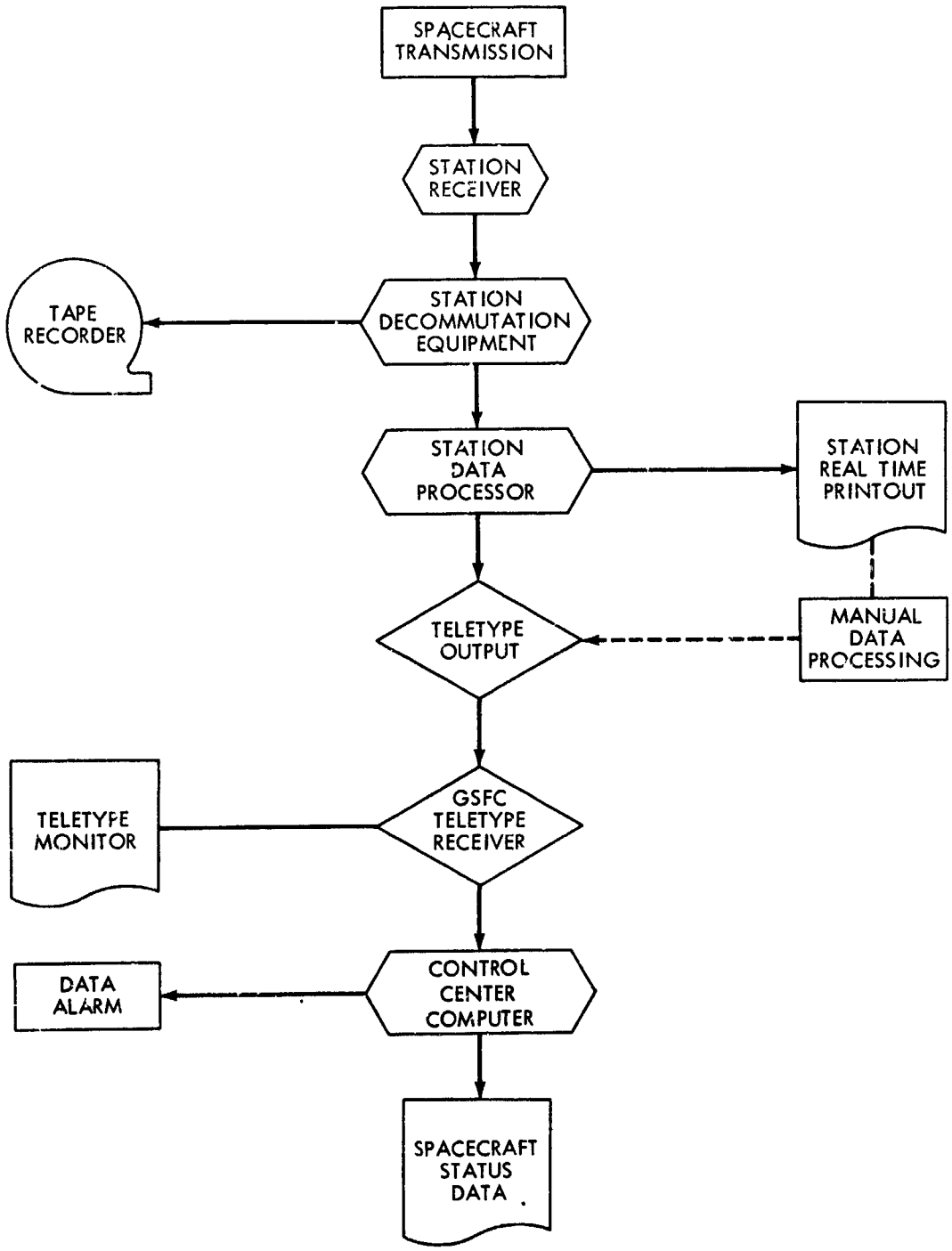

Figure 14. AIMP Real-Time Data Flow

installed on the launch vehicle. It is anticipated that the vehicle shroud will be installed on F-1 day. Spacecraft operations will be monitored at certain intervals during countdown up to liftoff.

Spacecraft Ground Support Equipment

Spacecraft test equipment is in five major categories:

- Experiment excitation source equipment: Light and radiation inputs, as well as current and count inputs, required to energize and test experiment sensors

- Spacecraft control and monitoring equipment: A blockhouse control unit, external power sources, meter control panel, high-accuracy voltmeters, etc., required to check out control functions, to monitor spacecraft power and power distribution, and to monitor spacecraft equipment response

- Spacecraft receiving and data-storage equipment: Circuitry for receiving, demodulating, and displaying the spacecraft phase-modulated carrier signal; equipment for measuring RF power; and tape recorders for storing data

- PFM buffering equipment: Extracts channel and frame synchronization information from telemetry signals; digitizes each channel; presents these data (in parallel binary form) with a channel tag to the data-reduction computer

- Real-time data-reduction equipment: For data collection, storage, conversion (to decimal numbers or engineering units), decommutation, decoding (frame-sequence information and condensed digital magnetic-tape data), and printout (either digital-magnetic-tape or real-time telemetry)

Telemetry Receiving System

The telemetry system uses the STADAN network standard equipment for receiving and recording telemetry data; however, other antenna systems having a 21-db or greater gain may be used. Special equipment required to reduce housekeeping and optical, aspect data in real time during the transfer trajectory, will be installed at selected sites to provide spacecraft status data to the project office. This information is necessary to determine the status of the spacecraft and the need for appropriate command action, to establish the spin-axis orientation and for use in determining retromotor firing time.

Transmitter output power will be 6 watts. The sideband power for a +57-degree phase-modulated signal is twice the carrier power, or 4 watts.

$$P_t = 36.0 \text{ dbm}$$

Transmitting antenna gain includes the dipole gain, wiring harness loss, and circular polarization loss.

$$G_t = -4 \text{ db}$$

Receiving antenna gain is based on the assumption that the 21-db gain array of crossed-yagi antennas (NASA 16) will be used.

$$G_r = +21 \text{ db}$$

Attenuation caused by the 250,000-nautical-mile maximum path loss is:

$$\frac{(\lambda)^2}{(4\pi r)} = \frac{300{,}000}{136 \times 10^6 \times 4\pi \times 2.5 \times 10^5 \times 1853}$$

$$= (3.80 \times 10^{-10})^2 = 14.4 \times 10^{-20}$$

$$= 1.44 \times 10^{-19}$$

$$= 1.6 - 190 \text{ db}$$

$$= -188.4 \text{ db}$$

Substitution of the above factors in the received power equation yields:

$$W_r = P_t + G_t + G_r \frac{(\lambda)^2}{(4\pi r)^2}$$

$$= +36.0 - 4 + 21 - 188.4 = 135.4 \text{ dbm}$$

$$= 2.9 \times 10^{-17} \text{ watts}$$

Safety Margin

Sky-noise temperature at 136 Mc in the plane of the ecliptic has an average value of about 600°K; however, there is a hot spot of about 2000°K looking toward the center of the galaxy.

The receiver-noise figure is 3 db, corresponding to a receiver-noise temperature of 290°K. The earth-generated noise temperature seen by the antenna sidelobes and the atmosphere noise is 55°K. The noise temperature then becomes:

$$T_n = 600° + 290° + 55° = 945°K$$

A set of 128 contiguous filters will be used in detection process during data reduction to enhance the output signal-to-noise ratio. The bandwidth of each filter is 100/16, or 6.25 cps.

The performance of the telemetry system can best be judged by knowing the probability of a word error as a function of a parameter independent of the detection process. This parameter, Pe, is the received energy per bit divided by the noise-power density P_n.

$$Pe = \frac{Wr \times T}{P_n \times n}$$

where

Wr = received power

T = time length of word

P_n = noise-power density

n = degree of coding

The power spectral density of the noise at the input to the receiver is given by

$$P_n = kT_n.$$

where

$$k = 1.38 \times 10^{-23} \text{ watt-seconds per degree}$$

$$P_n = 1.38 \times 10^{-23} \times 945 \text{ K}$$

$$= 13.0 \times 10^{-21} \text{ watt-seconds}$$

The parameter β becomes

$$\beta = \frac{2.9 \times 10^{-17} \times 0.16}{13.0 \times 10^{-21} \times 7} = 50.8 \text{ or } +17.1 \text{ db}$$

In Figure 15, a vertical line is drawn corresponding to a value of 50.8, or 17.1 db representing β for AIMP. At an error probability of one error in 1000 words, the safety margin for a perfect comb filter is therefore 12 db.

Information Processing

The AIMP data-handling system is designed to provide the experimenter with raw data from his experiment as soon as possible in the most useful format for analysis. The system employs high-speed electronic data-processing machinery (EDPM) and high-performance analog-to-digital conversion equipment to convert tape-recorded telemetry signals (representing either encoded digital data or continuous signal data) to a universal digital representation. The checking, editing, formatting, and separation of each individual experimenter's data is an internal operation of a medium-scale computer. The basic system output is a 556-bpi, 7-track magnetic tape compatible with IBM computers using binary-coded decimal formats suitable for algebraic compile language (such as FORTRAN) analysis.

Information Flow

The AIMP information will be converted to digital form by either the F8 STARS line now being completed or by the existing F5 line. The digital data are prepared by the AIMP edit program as a master-data tape, which in turn is used as the input to the decommutation program. The decommutation program separates individual experiment data from the commutated data train and recombines it to create individual experiment-data tapes.

Each experimenter's data will be accompanied by an accurate time reference and a calibration and scaling procedure (mathematical formula and error analysis), but no attempt will be made to return analog data to its original form.

The AIMP information-processing system will not merge the scientific data directly with the trajectory information, because of the requirement that trajectory and spin-axis information must undergo a series of modifications and refinements before use. This delay in trajectory and orientation information will not prevent experimenters from proceeding with the initial stages of analysis so long as an accurate time reference is provided.

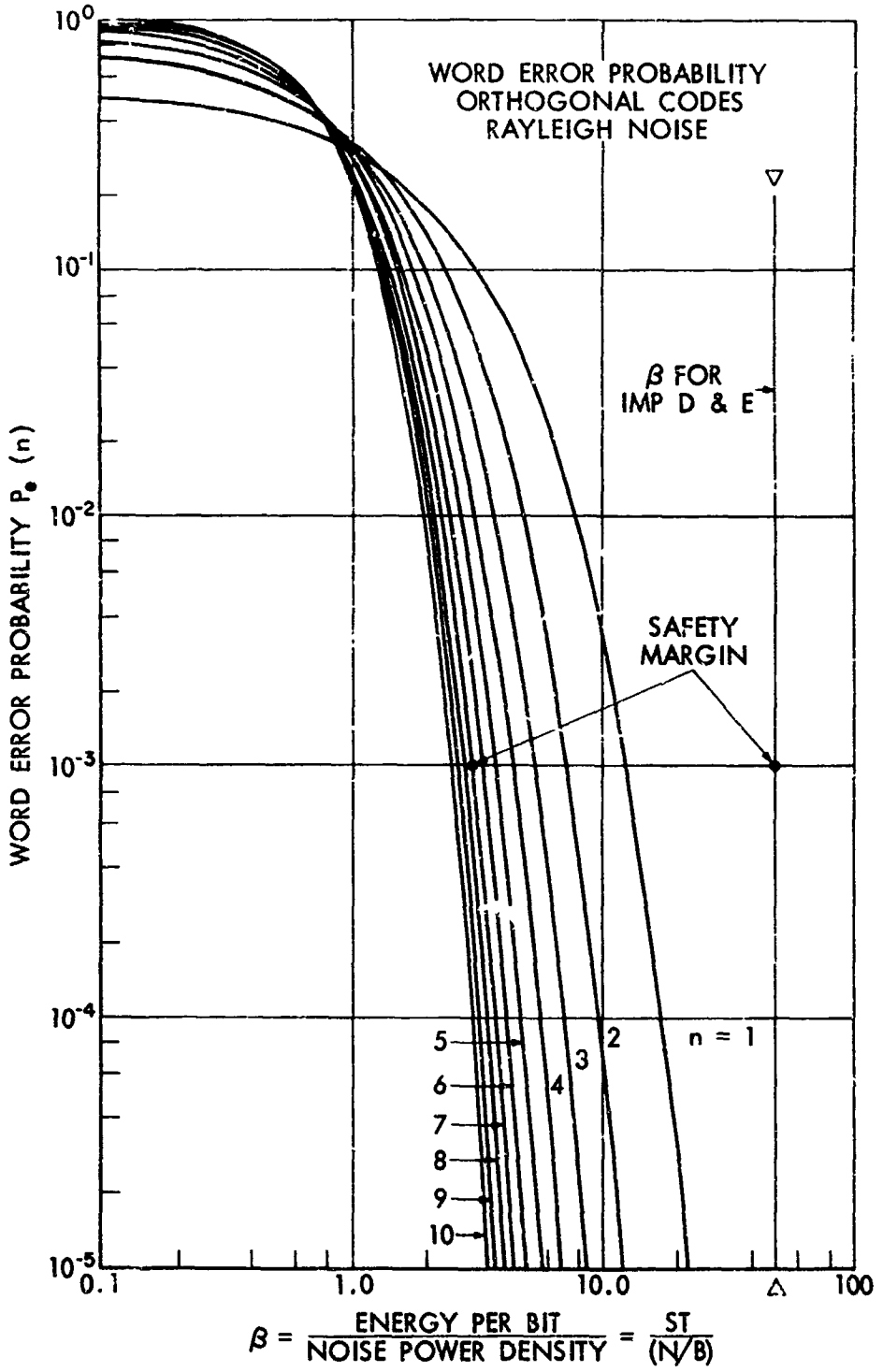

Figure 15. Word-Error Probability Curves for Rayleigh Noise

Experimenter Orbit Tape

An orbit tape containing the following data will be prepared for each experimenter:

- Moon position in celestial inertial coordinates
- Moon position in geocentric solar-ecliptic coordinates
- Moon position in geocentric solar magnetospheric coordinates
- Sun position in celestial inertial coordinates
- Spacecraft position in celestial inertial coordinates
- Spacecraft position in geocentric solar-ecliptic coordinates
- Spacecraft position in geocentric solar-magnetospheric coordinates
- Spacecraft position in selenocentric solar-ecliptic coordinates
- Spacecraft subsatellite position in geomagnetic latitude and longitude
- Spacecraft spin axis in inertial geocentric coordinates
- Spacecraft spin axis in geocentric solar-ecliptic coordinates
- Spacecraft spin axis in solar geocentric magnetospheric coordinates
- Spacecraft spin axis in selenocentric solar-ecliptic coordinates

The time interval at which this data is presented will be a function of the orbit achieved.

BLANK PAGE

RELIABILITY AND QUALITY ASSURANCE PROVISION

GENERAL

The AIMP project office, with the assistance of a reliability assessment contractor (Bird Engineering-Research Associates, Inc.), has made a preliminary review of all experiment and instrumentation subsystem and system designs, checking their component parts against a list of preferred spacecraft flight parts. Other reviews are scheduled at critical times in the schedule.

An experiment, instrument, or spacecraft hardware is considered flight-worthy primarily on the basis of the empirical data collected from a series of operational and environmental tests conducted on the specific experiment, instrument, or spacecraft hardware itself, and tests conducted on the complete spacecraft. The project office with the assistance of the reliability assessment contractor will review all failures during testing and take appropriate action.

All instrumentation and experiments are to be built to meet the AIMP Test and Evaluation Specification developed by the T & E Division at Goddard which are based on launch vehicle and orbit environments. Some experimenters have objected to the inclusion of any NASA Quality Publications (primarily NPC-200-3) as part of their contract; therefore, the use of such documents is limited in this project. All experimenters have agreed to keep a failure analysis record and report the failure of specific parts or components to the project office. Most experimenters have accepted the project office's offer to have the GSFC Quality Assurance Branch make a failure analysis for the experimenter on the parts that fail. GSFC Malfunction Report Form 4-2 (3-65) will be used within GSFC to report all known failures.

QUALITY CONTROL

Fabrication

The primary feature of this system is a thorough examination of each electronic card in each step of the fabrication process beginning with a general workmanship and magnetic materials inspection.

Decontamination

General—In general the electronic cards are to be delivered to GSFC unpotted. The experimenter or instrumenter must obtain a waiver from the project office for exclusion from this requirement or for including prepotted components as part of their electronics.

Inspection—All electronic cards will be inspected for workmanship, damage, and magnetic materials. All units received will be photographed. An inspection form will be filled out in quadruplicate: one copy to the originator of the card, one to the project office, one to file, and one to a master log kept on each specific unit.

Control Strips—Control strips (some populated with a known number and type of microorganisms, others sterile) will be placed on various sections of the spacecraft or components. Particles of these strips will be removed at appropriate times to check the effect of the decontamination procedures or the state of the spacecraft contamination.

Preliminary Decontamination—All decontamination procedures will take place inside a clean room. Electronic circuit boards will be brush-cleaned with xylene around the soldered connections, rinsed in an isopropanol alcohol bath, and baked at 55° C for 5 minutes. Then the cards will be placed in a fresh isopropanol alcohol (chemically pure C^3H^7 OH) bath for 5 minutes, after which the cards will be placed in a thermal-vacuum chamber where the pressure will be reduced to 1×10^{-3} mm Hg or less and the temperature held to 55° C, +0, -5° C for a minimum of 1 hour. At the end of this time the chamber will be back filled with dry nitrogen. The cards will then be removed and coated with a thin film (3 mil) of nonrigid epoxy. The cards will be inspected and photographed, and a conformal coating form filled out in quadruplicate. The cards will then be turned over to the integration team for reintegration with the spacecraft and temperature testing.

Potting—The cards will be returned to the decontamination group for potting after successful temperature testing. The alcohol bath and baking routine will be repeated. The cards will be reinspected and then encapsulated in a high temperature polyurethene closed cell foam. From this point, decontamination will be treated as a surface problem and the inspection will consist of examining connectors, frame, and potting material for mechanical damage. An encapsulating form is filled out in quadruplicate and then distributed.

Final GSFC Decontamination—The spacecraft will be taken into the GSFC clean room. All exposed parts will be wiped with alcohol and a general inspection made for mechanical damage. The control strips will be examined for the amount of contamination present on the spacecraft to determine the necessity for further decontamination procedures. The spacecraft will be placed in a sterile container for shipment to the clean room at ETR.